TR 63-475.4

HIGH TEMPERATURE PROTECTIVE COATINGS FOR REFRACTORY METALS

PART I - Development of Oxidation Resistant Coatings for Refractory Metals

L. Sama

PART II- Experimental Study of Factors Important in the Protection of Tungsten above 1900°C

C. D. Dickinson

SEVENTH MEETING OF THE REFRACTORY COMPOSITES WORK GROUP

Palo Alto, California — March 12-14, 1963

Sponsored By

The Aeronautical Systems Division, Materials Central

and

National Aeronautics and Space Administration

General Telephone & Electronics Laboratories Inc.

Bayside Laboratories, Bayside, New York

PART I

DEVELOPMENT OF OXIDATION RESISTANT COATINGS FOR REFRACTORY METALS

L. Sama

General Telephone & Electronics Laboratories Inc.
Bayside Laboratories, Bayside, New York

1. INTRODUCTION

The coating work being conducted at this laboratory consists of two parts: Part I is concerned with the practical development of coatings for all of the refractory metals and Part II is a more fundamental program which is directed toward clarification of factors of importance in coatings for tungsten above 1900°C. The objective of this portion of the report is to summarize the work in progress in Part I which covers a fairly broad spectrum of the refractory metals and alloys and, particularly, to give some of the highlights of results obtained on an Air Force-sponsored program [1] on several tantalum-base alloys.

---

[1] L. Sama, "Oxidation Resistant Coatings for Tantalum Alloys and Other Metals," TR-62-460.7 from General Telephone & Electronics Laboratories Inc. to ASD on Contract No. AF(657)-7339, January 1963

2. COATING DEVELOPMENT AND APPLICATION

The investigations can be divided into three areas: (1) in-house work, (2) Government-sponsored work, and (3) the coating of samples and hardware for outside company evaluation and use. A rather broad range of metals and alloys has been covered under these three programs. Both development and evaluation are continuing on a modified silicide coating for tungsten and tungsten alloys and molybdenum. A number of coatings have been developed or adapted for particular processing and operating conditions for columbium alloys. The coatings consisted of Sn-Al, Ti-Al, Ti-Si, and Ti-Cr-Si. Among the alloys investigated are B-66, X-110, D-14, D-36, D-31, FS-85, Cb-752, and a number of proprietary alloys for several companies. Molybdenum, TZM, and Mo-.5Ti have been coated with Sn-Al with certain modifications. Evaluation samples such as coupons, foil, and tensile bars have been prepared for evaluation. Hardware items such as nozzles, thrust chambers, power conversion devices, and jet engine parts have been coated for outside evaluation and use. Environmental conditions are usually oxidizing and the hardware coated has been evaluated in rocket propellant exhaust streams and in hydrocarbon fuel erosive environments. The types of coatings developed and evaluated, in addition to their varied

composition have also been diverse in their method of application. These consisted of slurries, hot dipping, pack cementation, and pack cementation plus hot dipping.

A year end report has been written covering the results of the development of oxidation-resistant coatings for the refractory metals which was sponsored by ASD. The report was fairly extensive and was concerned primarily with the development and evaluation of tin-aluminum slurry coatings for the refractory metals, particularly for tantalum-base alloys. Since the report was quite extensive and will receive rather wide distribution, only a few of the areas investigated will be touched on here.

An extensive evaluation of the effectiveness of the tin-aluminum spray slurry coating process was conducted on Ta-10W, Ta-30Cb-7 1/2V, and Cb-5 Zr. Some of the data covering stress rupture evaluations, oxidation tests, and reduced pressure environment tests are covered here for 0.040" thick Ta-10W and 0.020" thick Ta-30Cb-7 1/2V. The Ta-10W was coated with Sn-25Al and the Ta-30Cb-7 1/2V was coated with Sn-50(Al-Si). These coating compositions were modified by the addition of both tantalum and molybdenum powder plus excess aluminum to the slurry so that during the subsequent diffusion treatment intermetallic particles were formed, which provided a network for preventing a run-

off of the excess Sn-Al phase. All samples were spray coated with the slurry and then vacuum diffused at 1850°F approximately for 1/2 hour; the process was repeated to build up the coating thickness.

Short time stress rupture data are shown in Fig. 1 for both alloy materials. Data taken from literature for Ta-10W tested in vacuum at the same temperatures are plotted for comparison. At the time of writing, no equivalent data for the Ta-30Cb-7 1/2V tests at 2700°F were available for comparison. The data obtained here for the Ta-10W coated samples at 3000°F appear to fall between two sets of data obtained by other investigators in vacuum tests at 3000°F. The 2800°F data obtained here fall quite close to that plotted from the literature. The stress rupture strength of the Ta-Cb-V alloy is much lower than the Ta-10W, even though the ternary alloy data were obtained at a lower temperature. In fact, the slope of the curve is quite steep for the Ta-Cb-V alloy at 2700°F, and if extrapolated to a 100-hour rupture life, the stress would be about 2000 psi. However, if the data were plotted on a strength-to-weight ratio basis, the Ta-Cb-V alloy would show up much more advantageously. The deformations involved in all cases were quite considerable, amounting to as much as 30 to 40%. Therefore some of the coating tended to chip off or flake off, particularly in the last stages of rupture. However, the only visual evidence of oxidation occurring at or in the vicinity of fracture in these and other

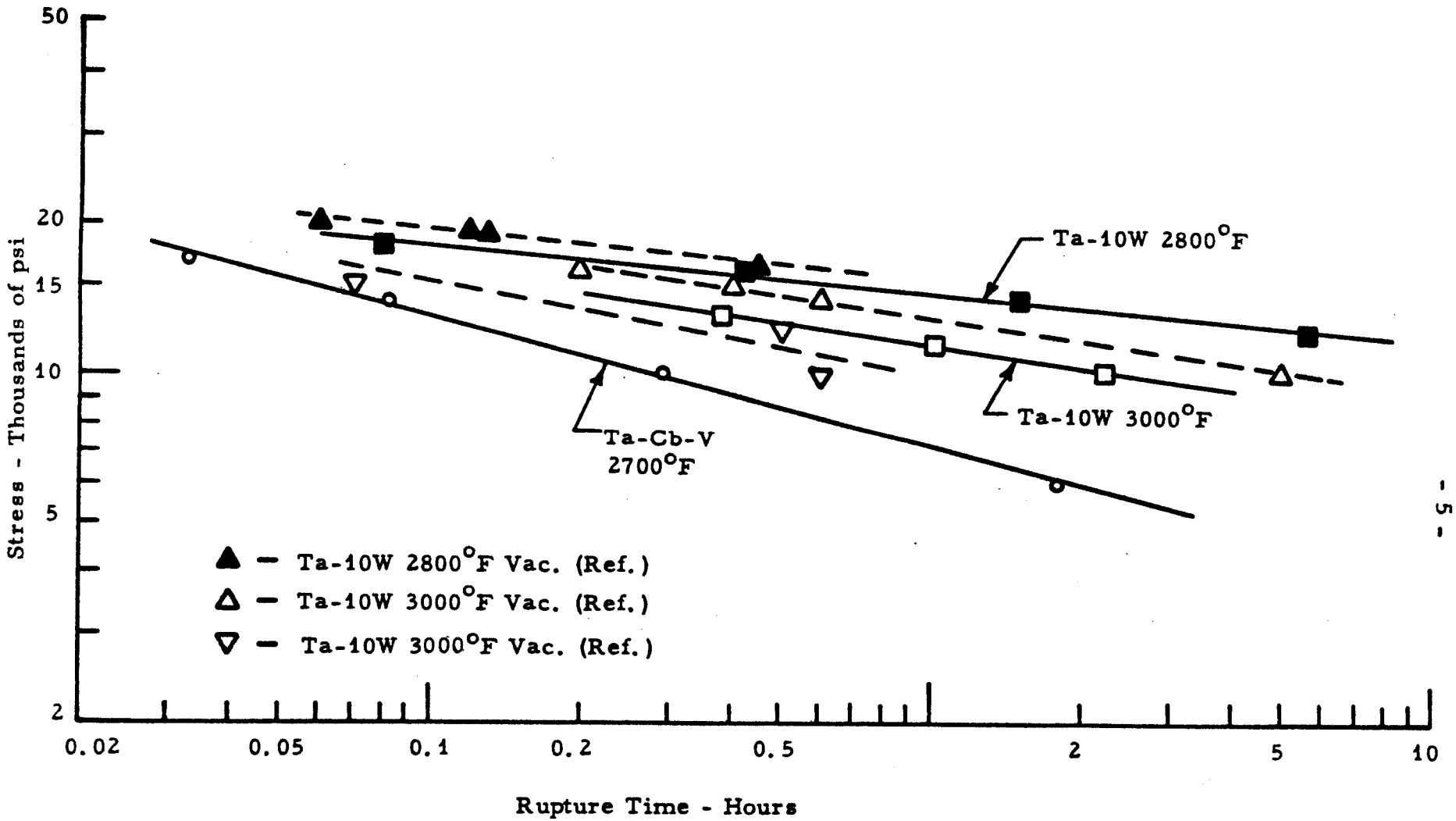

Fig. 1. Stress-rupture curves for Ta-10W and Ta-30Cb-7.5V coated samples tested in air.

tests was in the Ta-Cb-V alloy tested for the longest time, and this was at the tip of the fracture.

Similarly coated coupon samples of each alloy were also tested in batches at tempertures from 1100 to 3000°F in furnaces. Some of the 2500 to 3000°F data are shown here. Life in hours vs. coating weight are plotted in Figs. 2 and 3 for the Ta-10W alloy and in Fig. 4 for the Ta-Cb-V alloy. It was found, in general, that substrate thickness, size, or edge rounding had little effect on oxidation resistance. The most significant effects were due to coating thickness and cycling rate. Failures occurred predominantly at edges at all temperatures. At 3000°F with Ta-10W, oxidation life increases slightly with increased coating thickness. Little effect of sample size is indicated between 3/4" and 1-1/2" long samples. Samples given only one coating had respectable lives of 3 to 6 hours. At 2800°F there was practically a linear relationship between the coating thickness and oxidation life. In fact, the major effect of the molybdenum additive over tantalum is clearly to increase the coating thickness and the data fall in line with the thinner coatings. It can also be seen that the cycling rate has a profound effect on life at 2800°F. In reducing the cycling rate to once a day, lives over 75 hours were obtained.

For the Ta-Cb-V alloy at 2500°F there was a very sharp increase in life with coating thickness. The first batch of samples had lives varying from 40 to over 85 hours. With somewhat thicker coatings

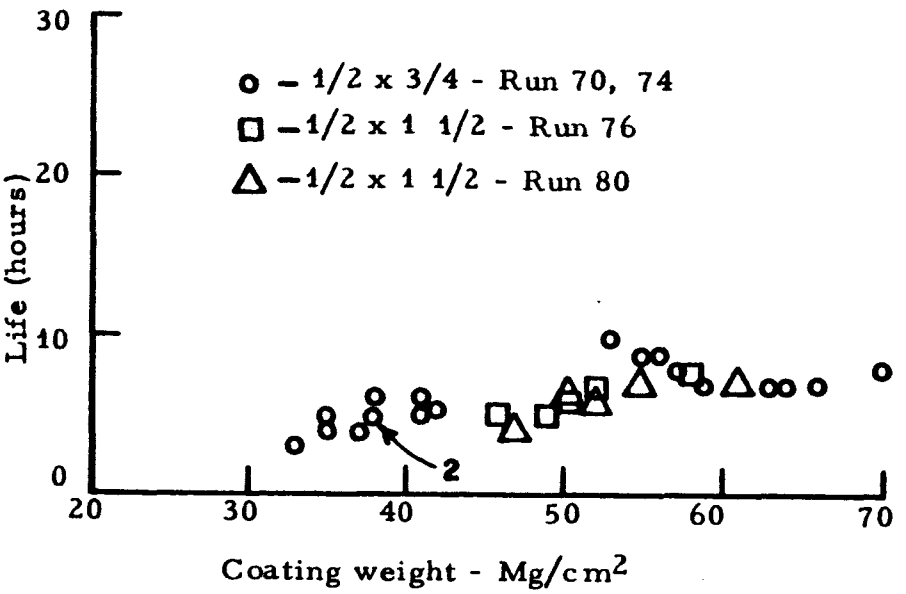

Fig. 2. Oxidation life in furnace tests of Ta-10W samples coated with (Sn-25Al)-10$TaAl_3$ and tested at 3000°F.

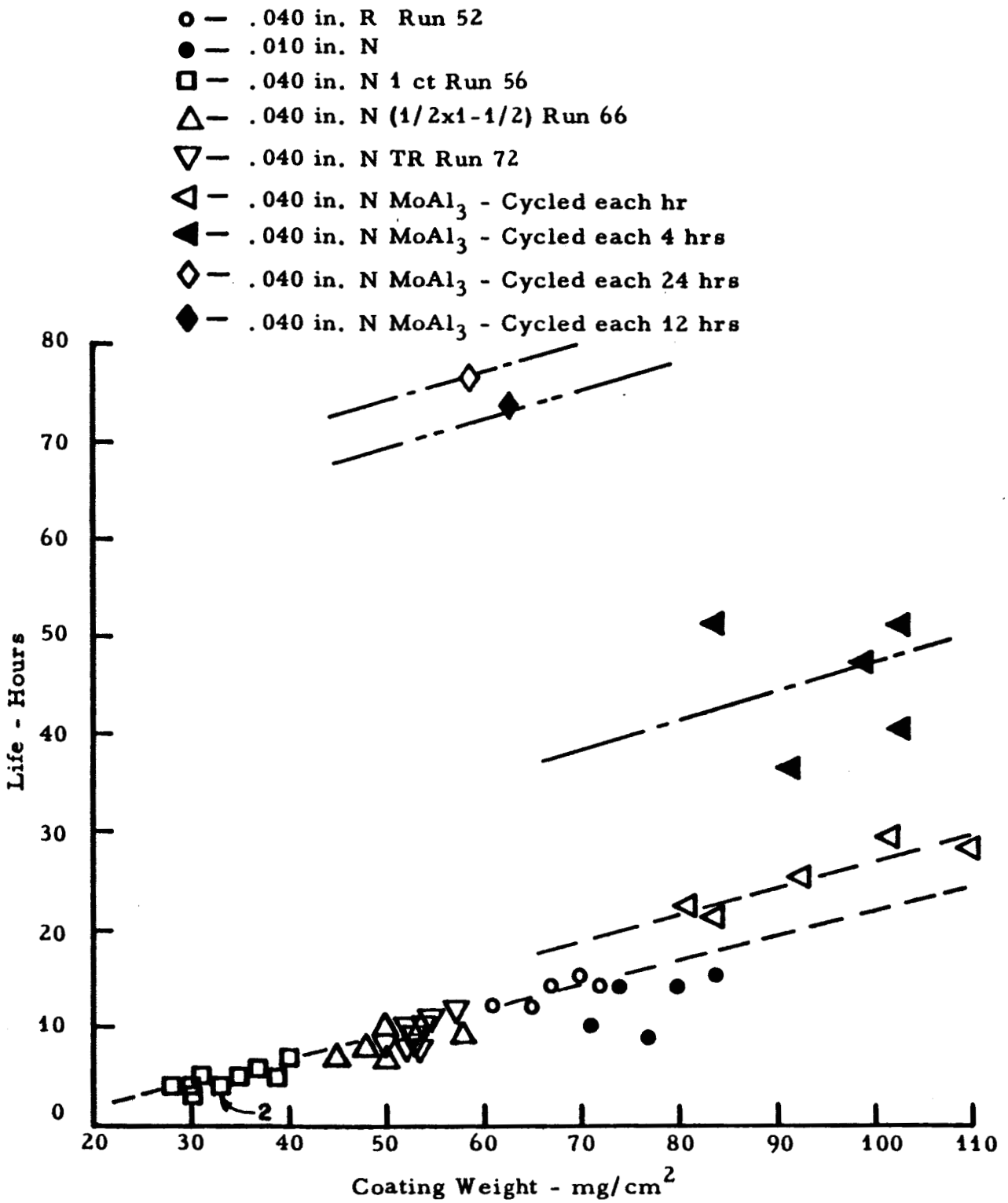

Fig. 3. Oxidation life in furnace tests of Ta-10W samples coated with (Sn-25Al)-10$TaAl_3$ and (Sn-25Al)-10$MoAl_3$ and tested at 2800°F.

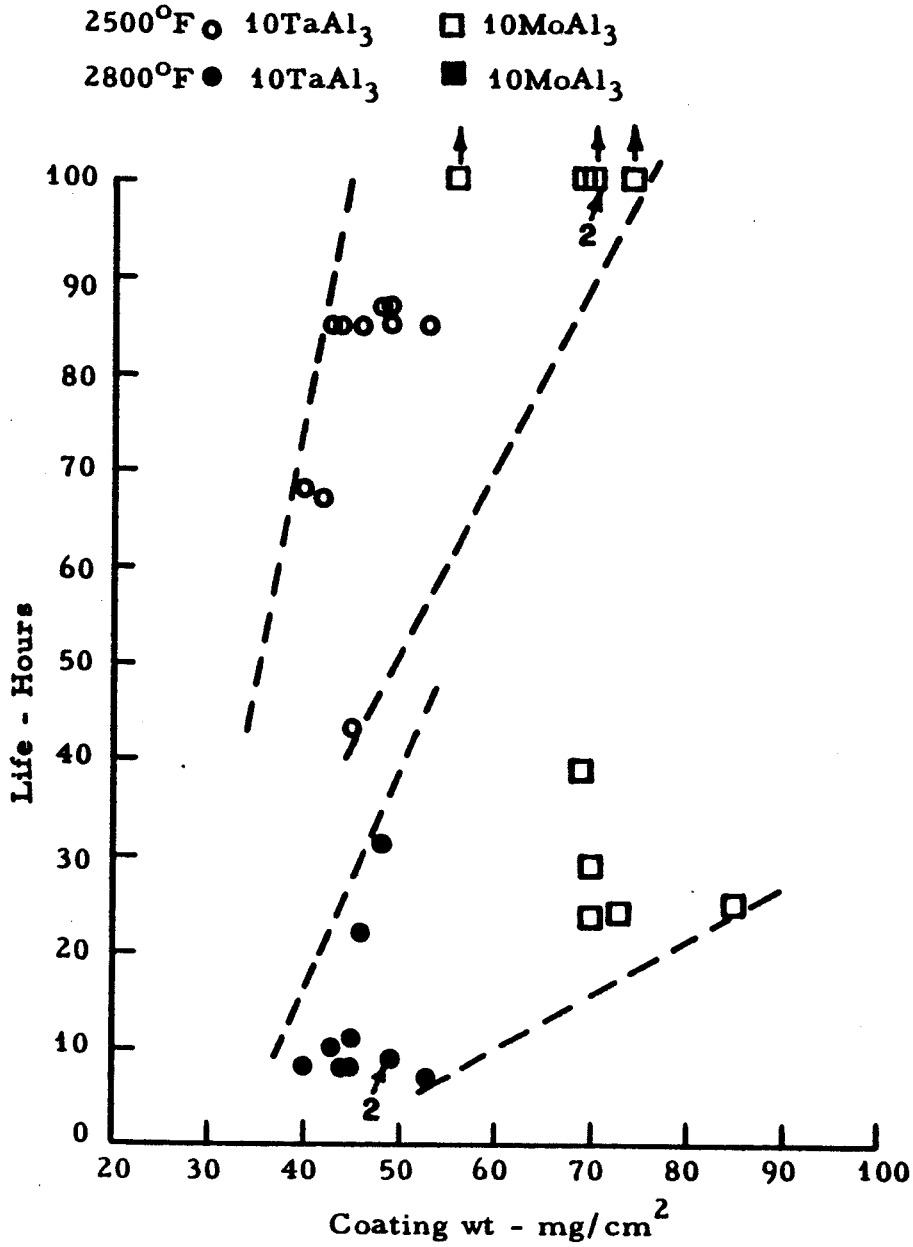

Fig. 4. Oxidation life of Ta-30Cb-7.5V coated samples at 2500 and 2800°F.

provided by the addition of 10% molybdenum powder to the coating, none of the five samples tested failed in 100 hours at 2500°F. At 2800°F most of the samples failed in 7 to 11 hours, with several lasting up to 30 hours. Coating thickness did not appear to have any particular effect in the range studied. However, the batch of samples with the molybdenum additive had considerably thicker coatings and had longer lives of 24 to 39 hours. In general, the coatings are much thicker than those with equivalent coating weights in the (Sn-25Al)-10$TaAl_3$ composition.

Much more extensive data are given in the final report concerning tensile strength, diffusion effects, and oxidation resistance of coated samples over a wider temperature range.

To study coating stability in the range of 1 to 15 mm of air pressure, a modified Sieverts apparatus was set up together with a resistance heating chamber. A cartesian manostat was used to regulate air pressure in the range of interest. Various attempts were made to minimize the temperature gradient resulting from clamping the specimen in water-cooled electrical grips. Initially this was done by contouring the sample so that the grip ends were narrowest and the sample widened gradually to a maximum of 1/4 in. at the center. Samples of Ta-10W, from 0.01 in. to 0.04 in. thick by approximately 2 in. long were coated with (Sn-25Al)-10$TaAl_3$. Tests showed, however, that the coating thickness variations within the sample test section were sufficient to cause a temperature gradient

in the sample. Therefore, subsequent samples were coated with the molybdenum additive to obtain much more uniform coatings. Additional difficulties were encountered because of the relatively small grip ends which led to hot spots and poor contact. This difficulty was alleviated by using completely rectangular samples, 0.010 in. thick x 1/4 in. wide, but the restraint imposed by the vacuum seals around the grips caused these samples to buckle at the center. In some cases this resulted in shorting out against the wall of the chamber.

Samples were usually exposed for 1/2 hour at temperature, taken out, examined, weighed, reassembled into the apparatus, and re-tested for another 1/2 hour. Many of the samples developed hot spots in some localized area, which resulted in a burnout. Therefore it was not possible to specify the type of failure that occurred. Accordingly, the results plotted in Fig. 5 are those for which a uniform weight loss or weight gain was obtained. None of these samples had failed in the classical sense of an oxidation failure. In fact most of them suffered little change in structure or appearance. It is apparent, however, that at 1.5 mm pressure considerable coating loss occurs in the vicinity of 2570°F in 1/2 hour. Similar losses are obtained at a lower temperature, 2450°F, in one hour. It can be seen from Fig. 5 that the coating is quite stable at approximately 2600°F at 3 mm pressure, at 2780°F at 6 mm pressure, and at 2850°F at 12 mm pressure. The effect of time at temperature is shown in

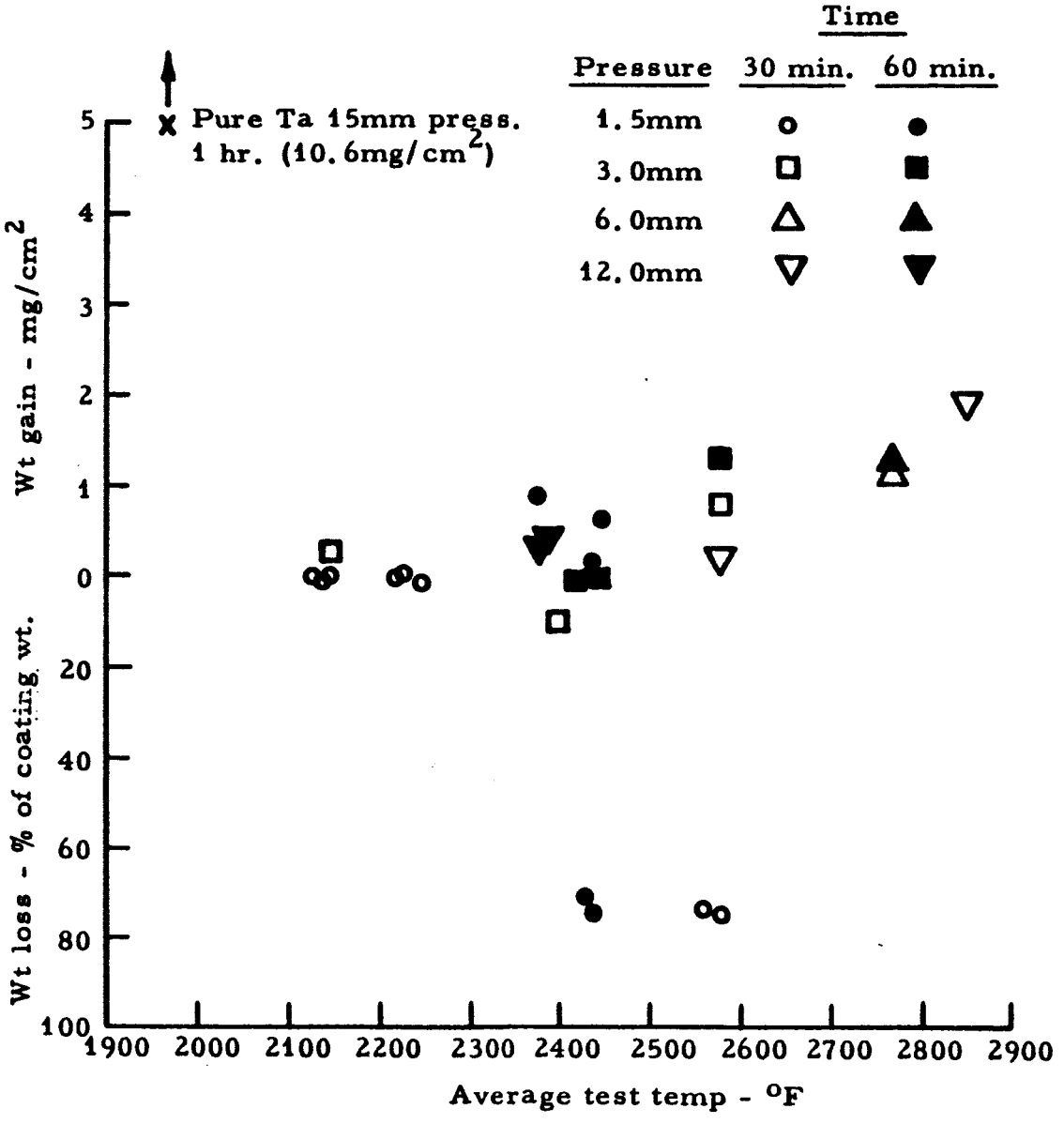

Fig. 5. Weight changes in coated samples at reduced air pressures.

Fig. 6. Where weight gains occur they appear to be continuous. From microstructural changes at 2700°F in 1 1/2 hours it is apparent that local areas can be depleted of the coating within this test time; these depleted areas are probably related to the hot spots within the sample caused by nonuniformities. In order to establish the range of pressures and temperatures at which the coating is stable, it would be preferable to use an outside heating source to attain necessary temperatures.

These studies indicate that where a protective oxide film forms, stability is increased and can probably be increased to temperatures in the vicinity of 3000°F. However, considerably more work would have to be done in order to establish the precise temperature-pressure boundary conditions for stability.

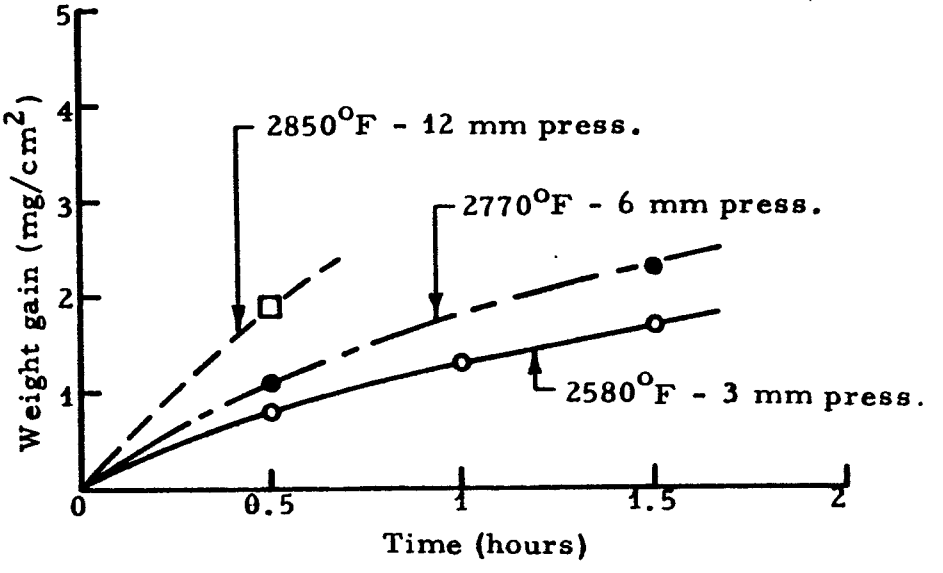

Fig. 6. Weight gains of samples of Ta-10W coated with (Sn-25Al)-10$MoAl_3$ and heated by their own resistance.

PART II

EXPERIMENTAL STUDY OF FACTORS IMPORTANT IN THE PROTECTION OF TUNGSTEN ABOVE 1900°C

C. D. Dickinson

General Telephone & Electronics Laboratories Inc.
Bayside Laboratories, Bayside, New York

1. INTRODUCTION

Silicide and aluminide-base coatings which adequately protect the refractory metals at temperatures up to 1900°C have a maximum upper temperature limit for protection of about 1900°C. Therefore, knowledge of the growth of protective films of more refractory, less volatile oxides has been the impetus behind investigation of the factors which are important in the growth of refractory oxides as a protective barrier for tungsten. An analysis of the problem was presented at the last Composites Work Group Meeting and five factors were discussed which seem to control the over-all efficacy of a barrier coating of oxide grown from a reservoir coating substrate. A detailed description of analysis of these five factors is given in Ref. 1, 2, 3, and 4 . The survey revealed that there were many areas in which information was insufficient and in which a better understanding would aid in the development of high-temperature coatings. So many areas requiring further study were revealed that some order of priority was required if significant assistance is to be given to development programs

now in existence or projected for the near future. The next objective, therefore, was to define the type of research programs needed and then to assign an order of priority.

Recommendations were made for specific experimental research programs needed to define each of the processes discussed in Ref. 3. The relative importance of these programs was evaluated in terms of the contribution that additional knowledge or information about the particular phenomena could make to coating development programs [4]. It is worthwhile, therefore, to briefly reiterate the five phenomena defined by the analysis of the problem being of major importance and to indicate their relative importance in determining the protectiveness of a coating system.

These phenomena are:

1. The breakaway proneness of the oxide formed.
2. The diffusion paths followed in the ternary oxygen-metal-metal coating environment system.
3. The rates of vaporization of the components of the coating system.
4. The rate of coating-substrate reactions.
5. The rates of cationic and anionic diffusion through the outer oxide layer.

In the final analysis, multicomponent diffusion processes and breakaway are the principal phenomena that initially determine if a coating

is protective, since protection depends on whether refractory oxides of the desired composition and structure are formed as an adherent non-porous film that grows by a diffusion controlled process. Predictions based on the existing knowledge in these two areas should be tested by critical experiments. For example, a demonstration that either the strength or ductility of a substrate affects the high-temperature film-forming characteristics of refractory oxides such as ZrO_2 and HfO_2, or changes the conditions for breakaway, would be an important step toward the better understanding and control of breakaway during the oxidation of refractory and intermetallic compounds. The influence of stoichiometry, as predicted by ternary diffusion, on the oxide formed has important implications for attempts to grow complex refractory oxides, and should be tested. Therefore, experiments have been conducted to provide additional insight on the processes of breakaway and ternary diffusion in oxidation which lead to the formation of refractory oxide films. The results of two experimental studies will be discussed separately in the following sections.

2. STUDY OF BREAKAWAY

The change to linear oxidation rates in the growth of refractory oxides such as Zr and Hf on their own substrate is generally associated with spalling and mechanical cracking of the oxide. Although a variety of

specific mechanisms for breakaway oxidation of individual metals have been proposed and are being investigated, a common denominator is that stresses or strains at the metal-oxide interface seem to be associated with breakaway phenomena in many systems. Therefore, an experimental program was designed to determine if the use of a liquid substrate could prevent breakaway in the growth of various refractory oxides by preventing the transmission of stress or strain from the substrate to the oxide. Achievement of this objective would have some practical implications, since the work of Sama [5] demonstrated that a liquid carrier layer can be used effectively in the formation of Al_2O_3 from coatings on the refractory metals.

2.1 PROCEDURE

The procedure used in the experimental work to be discussed is given in detail in Ref. 4 and will not be repeated. The general experimental procedures used were to melt an alloy of the desired composition in a zirconia or alumina crucible, machine the exposed metal surface and oxidize the sample in the crucible. Temperatures from 900 to 1700°C for various times were used to determine the kinetics of growth by weight gain and thickness measurements. Microprobe and X-ray analyses of the oxidized samples were used to identify specific phases observed metallographically. In all cases, oxides of the diluent used to produce a liquid phase alloy had a lower free energy of formation than the reactive element oxide. Tin and

gold were used as diluents. The growth of HfO_2 and ZrO_2 from a Hf or Zr alloy substrates were studied, using both tin and gold as a diluent. Growth of ThO_2 and Al_2O_3 from Th and Al alloys were investigated, using only tin as a diluent. Study of the oxidation kinetics of the six-liquid alloy system has been completed. Although certain peculiarities in behavior were observed which are characteristic of a specific system, the results which are described in the following section provide information with general implications on the effect of liquid substrates in the growth of refractory oxides without breakaway.

2.2 RESULTS AND DISCUSSION OF RESULTS

The effect of time and temperature on the rate of growth of oxides on Sn-16.7%Hf, Sn-9.3%Zr, Sn-5.3%Th and Sn-16.7%Al alloys are given in Figs. 1 to 4. The resulting curves are a plot of the specific weight gains or metallographically observed thicknesses as a function of the square root of the time of oxidation test. It will be observed in these figures that deviations from parabolic growth do eventually occur at many temperatures at longer times. The oxide films formed (Fig. 5) are compact and adherent at temperature. However, in certain systems, particularly the Au-Zr and Au-Hf systems, stresses generated on cooling caused the oxide to spall after the test had been completed. Even in the cases where the oxides had spalled on cooling, the weight gains indicated that protective growth had occurred during the isothermal test.

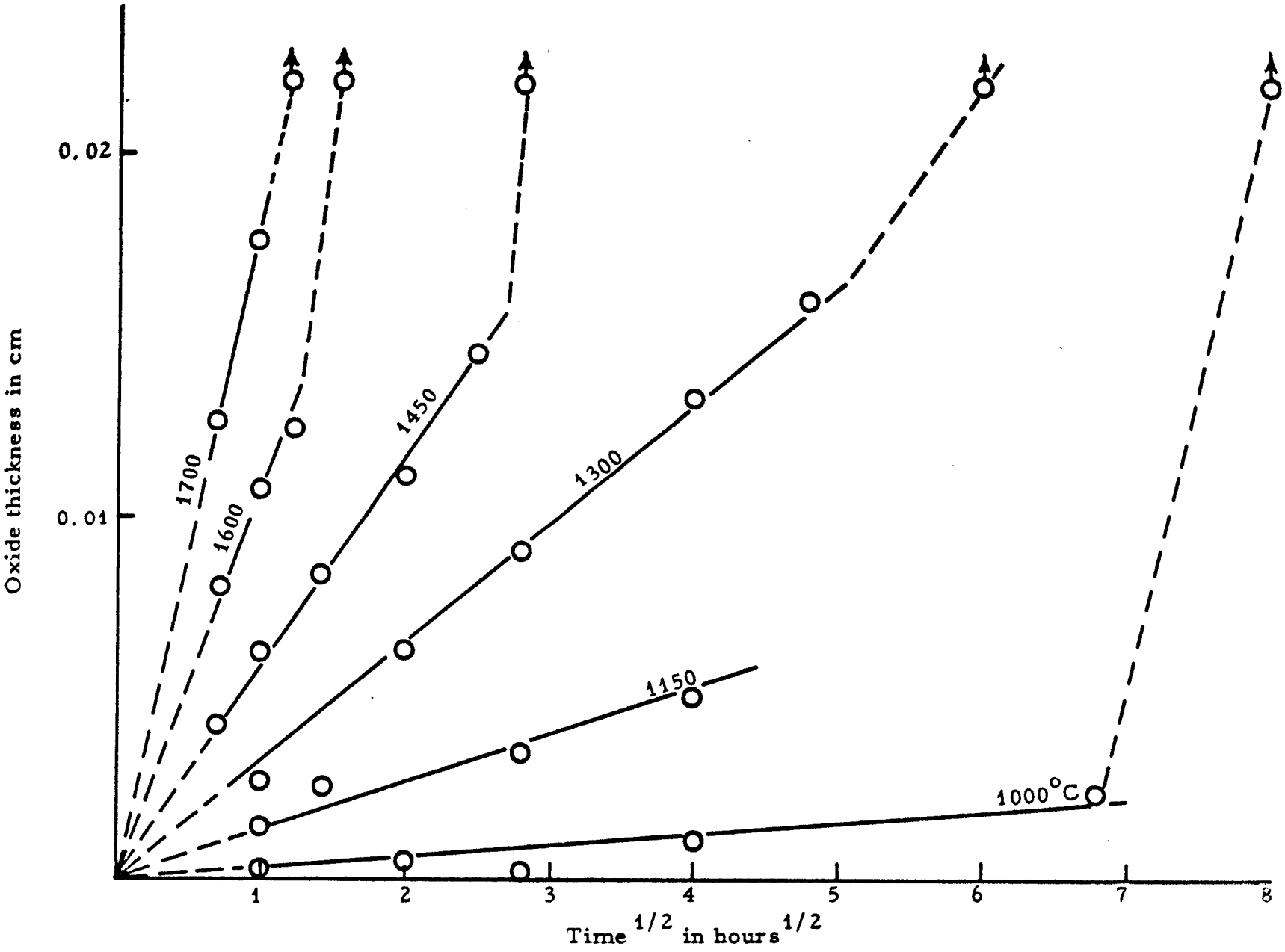

Fig. 1. The thickness of surface films formed on 16.7 w/o Hf-Sn alloy samples in dry air expressed as a function of oxidation time and temperature.

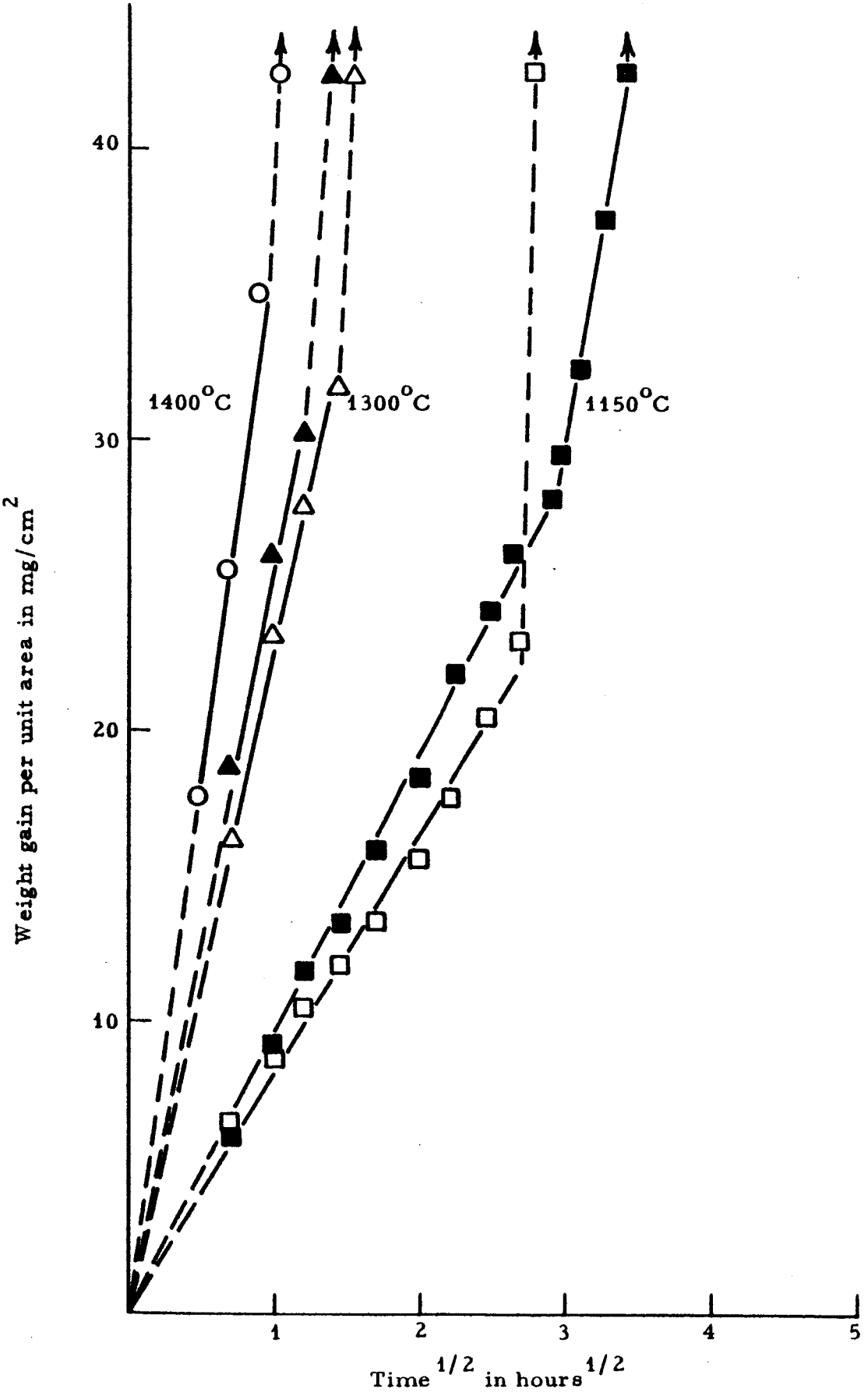

Fig. 2. The weight gains in dry air of 9.3 w/o Zr-Sn alloy samples expressed as a function of oxidation time and temperature.

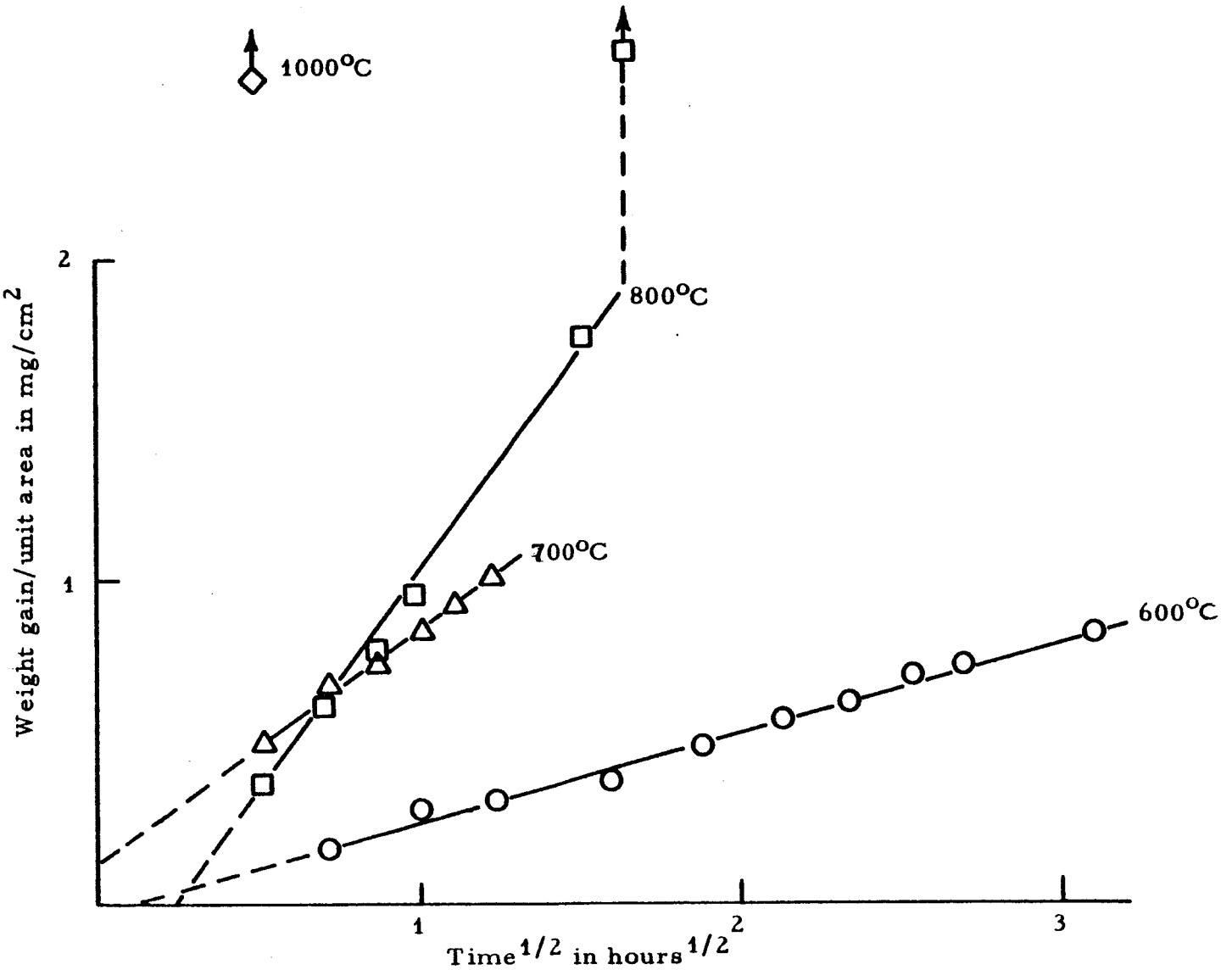

Fig. 3. The weight gains of samples of 5.3 w/o Th-Sn exposed to air, expressed as a function of time and temperature.

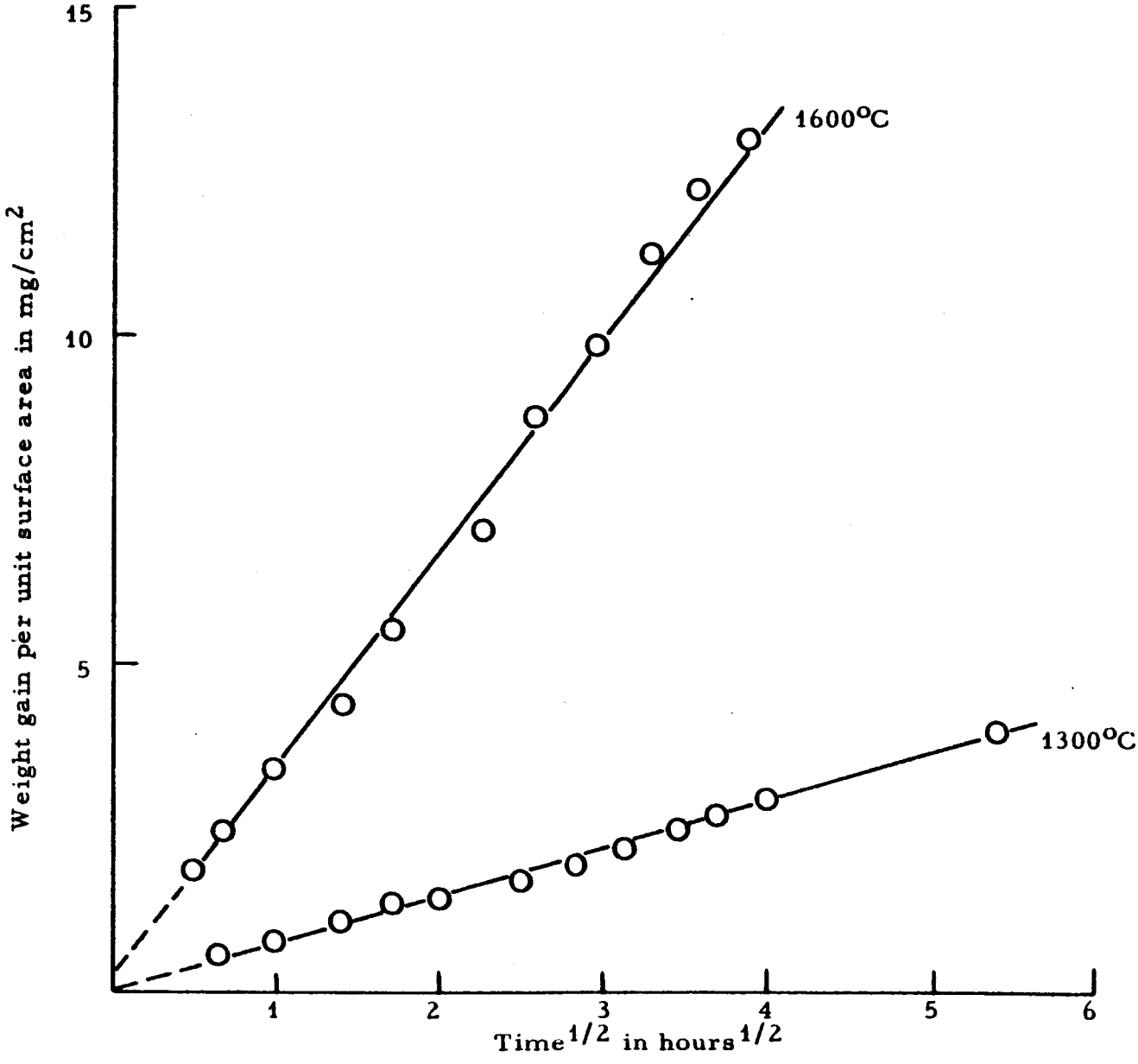

Fig. 4. The weight gains of samples of 16.7 w/o Al-Sn exposed to air, expressed as a function of time and temperature.

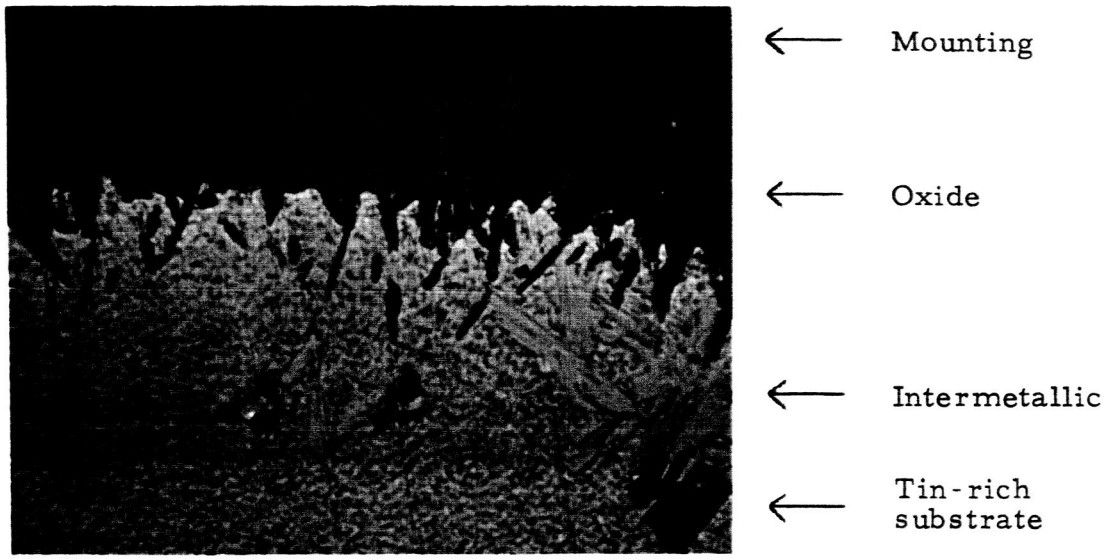

Fig. 5a. The surface of a 16.7 w/o Hf-Sn alloy sample exposed to air for 8 hours at 1150°C. (500X)

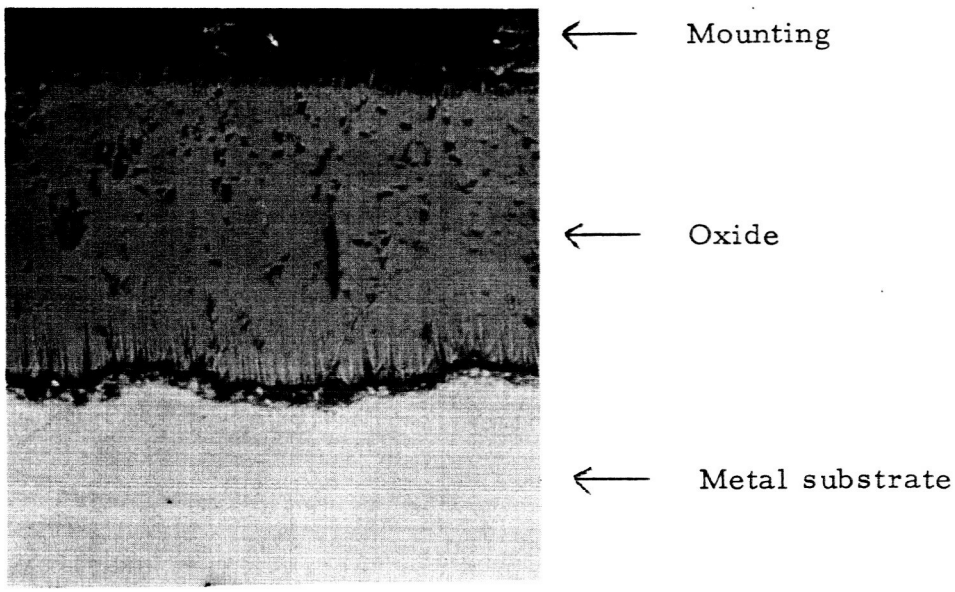

Fig. 5b. The surface of a 16.7 w/o Hf-Sn alloy sample exposed to dry air for 6 hours at 1450°C. (300X)

A comparison was made of the time for breakaway of the oxides on the liquid metal substrates with those reported in the literature for the growth of oxides on the solid, pure reactive metal, and the results indicate that a significant improvement at all temperatures in the time for breakaway resulted from the use of a liquid substrate. Microprobe or X-ray analyses indicated that the oxide formed during the parabolic period of growth was pure HfO_2, ZrO_2, ThO_2 or Al_2O_3. Furthermore the crystal form of the HfO_2 and ZrO_2 formed from Hf and Zr-containing alloys was monoclinic rather than cubic or tetragonal. Therefore, the parabolic growth and the fact that growth of the oxides is less prone to breakaway on the liquid substrates is a direct result of the elimination of stresses at the metal-oxide interface rather than an effect of alloying in the oxide.

Ultimately, however, breakaway does occur. Even though parabolic growth of HfO_2 for one hour at 1700°C is a marked improvement, much longer periods of protective growth will be needed if HfO_2 is to be a component of high-temperature coating systems. It is important to know the cause of the breakaway that occurs ultimately and hence to know whether the data obtained represent the best improvement that can be attained.

Breakaway during the oxidation of reactive-metal tin-base alloys manifests itself by the appearance of a white crumbly mass of tin oxides. The appearance of this other oxide could be the result of two processes; the mechanical breakdown of the protective HfO_2, ZrO_2 and ThO_2 films or

the exhaustion of the reactive metal in the sample by the formation of a thick oxide scale so that further oxidation results in the formation of tin oxides. This second process is believed to be operative on the basis of our experimental data. The times at which the concentration of the dispersed phase in hafnium-tin samples became zero (Fig. 6) were in excellent agreement with the times at which the crumbly oxide was first formed. The microprobe studies showed that hafnium was virtually insoluble in tin at room temperature; therefore all the hafnium content of the samples must have been in the dispersed phase and the times for zero concentration correspond to zero hafnium content.

If reactive metal exhaustion is assumed to be the case of breakaway, the time at which it occurs can be calculated readily. Since oxidation initially proceeds parabolically, the time at which breakaway occurs, t_B, should be related to the initial reactive metal content, m, by the expression

$$(m \times C) = k^{1/2} \; t_B \; ^{1/2} , \qquad (1)$$

where

C is the weight gain/unit area or film thickness produced by the consumption of one gram of reactive metal.

A comparison of the observed times at which the Sn-16.7w/oHf samples underwent breakaway with those predicted by Eq. (1), Table I, reveals a good agreement for all temperatures above 1000°C.

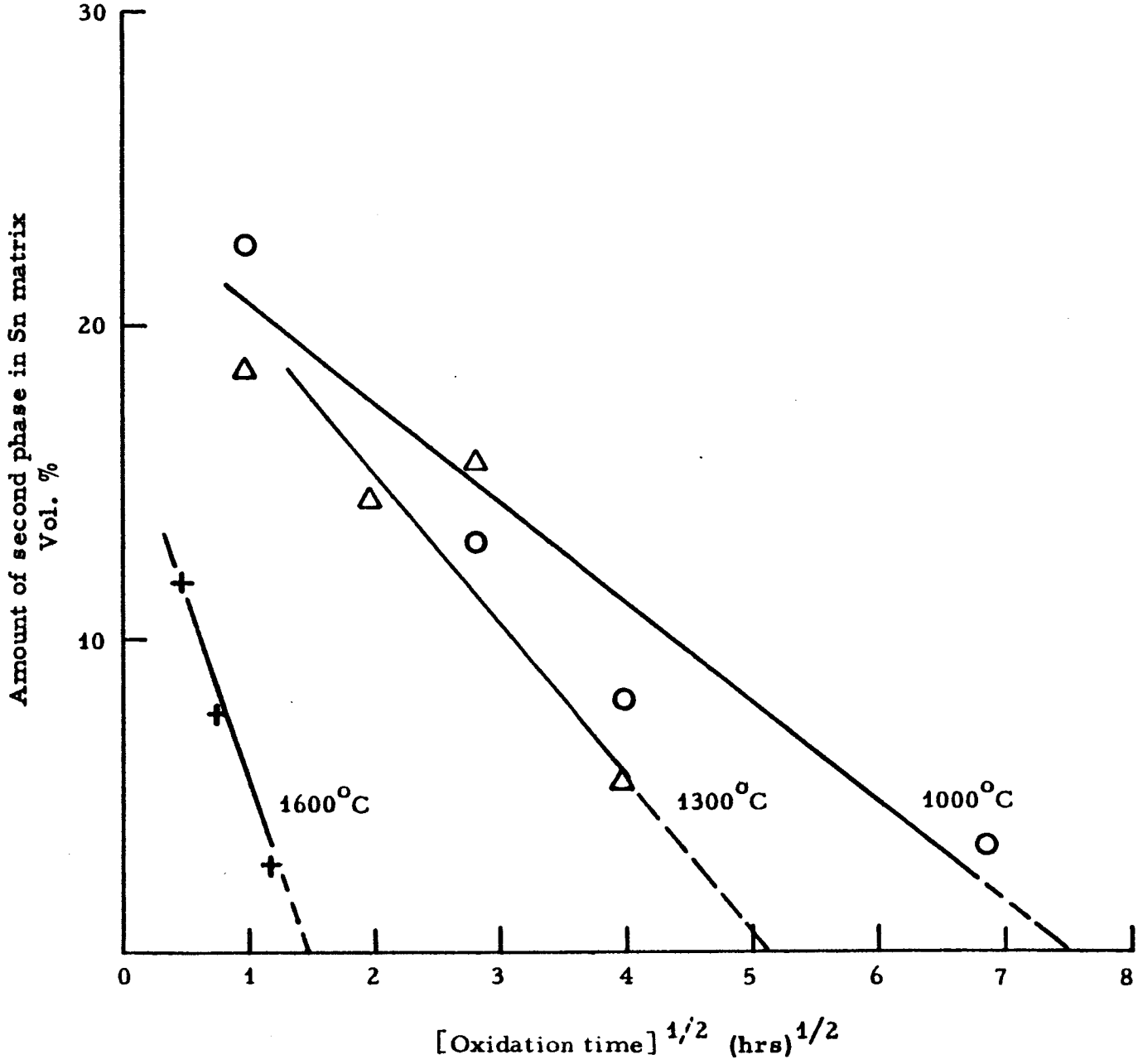

Fig. 6. The effect of oxidation time and temperature on the concentration of the dispersed phases present in samples of a 16.7 w/o Hf-Sn alloy.

TABLE I

The Times at Which Rapid Oxidation of Sn-16.7Hf Alloy Samples Commence

Temperature °C	Observed time * (hours)	Calculated time ** (hours)
1000	46-64	440
1150	-	170
1300	24-36	28
1450	6-8	7.4
1600	1.5-2	2.1
1700	1-1.5	0.9

* Taken from Fig. 8.

** Calculated from Eq. (1) using the average surface area of 14 cm^2. The rate constants were derived from the data presented in Fig. 1.

The good agreement demonstrated by the table provides strong confirmation for the suggested influence of reactive metal content. Further support comes from the fact that data on the effect of zirconium content on breakaway time obey one parabolic relationship over most of the zirconium content range evaluated, and breakaway is related to the initial zirconium content rather than being thickness or time dependent.

Deviations from the suggested parabolic relationship, however, do occur. The cause of the deviation at zirconium contents of 20 w/o or more

is probably due to the existence of solid islands of the zirconium-rich inetermetallic at the oxidation temperature of 1300°C. As shown by the oxidation behavior of the Sn-9.3w/oZr samples at 990 and 1030°C (Fig. 7), the oxidation rate is very high when the solid intermetallic is present and continues to be so until the solid is destroyed. This initial rapid oxidation rate causes an initial rapid depletion of the reactive metal and hence leads to an earlier onset of breakaway. This behavior is believed to be general and not specific to zirconium-tin since breakaway also occurs unusually early for Sn-16.7w/oHf samples oxidized at 1000°C, a temperature at which solid islands of hafnium-rich intermetallic are believed to be present. With the qualification that no solid reactive intermetallic is exposed to the oxidizing environment, the data indicate quite clearly that the times and temperatures for the onset of rapid linear oxidation in Figs. 1 to 3 do not represent the best that can be attained.

This program was not intended to be a study of the oxidation kinetics of tin alloys, but a certain amount of kinetic data have been obtained. It has been suggested that the use of liquid substrates prolongs the low temperature protective growth of the HfO_2, ZrO_2 and ThO_2, and, therefore, it would be interesting to compare the kinetic data obtained in this program with that reported for the protective growth of these oxide films on their parent metals at low temperatures. This comparison is best made in terms of the rate constant, k, which can be derived from the equation

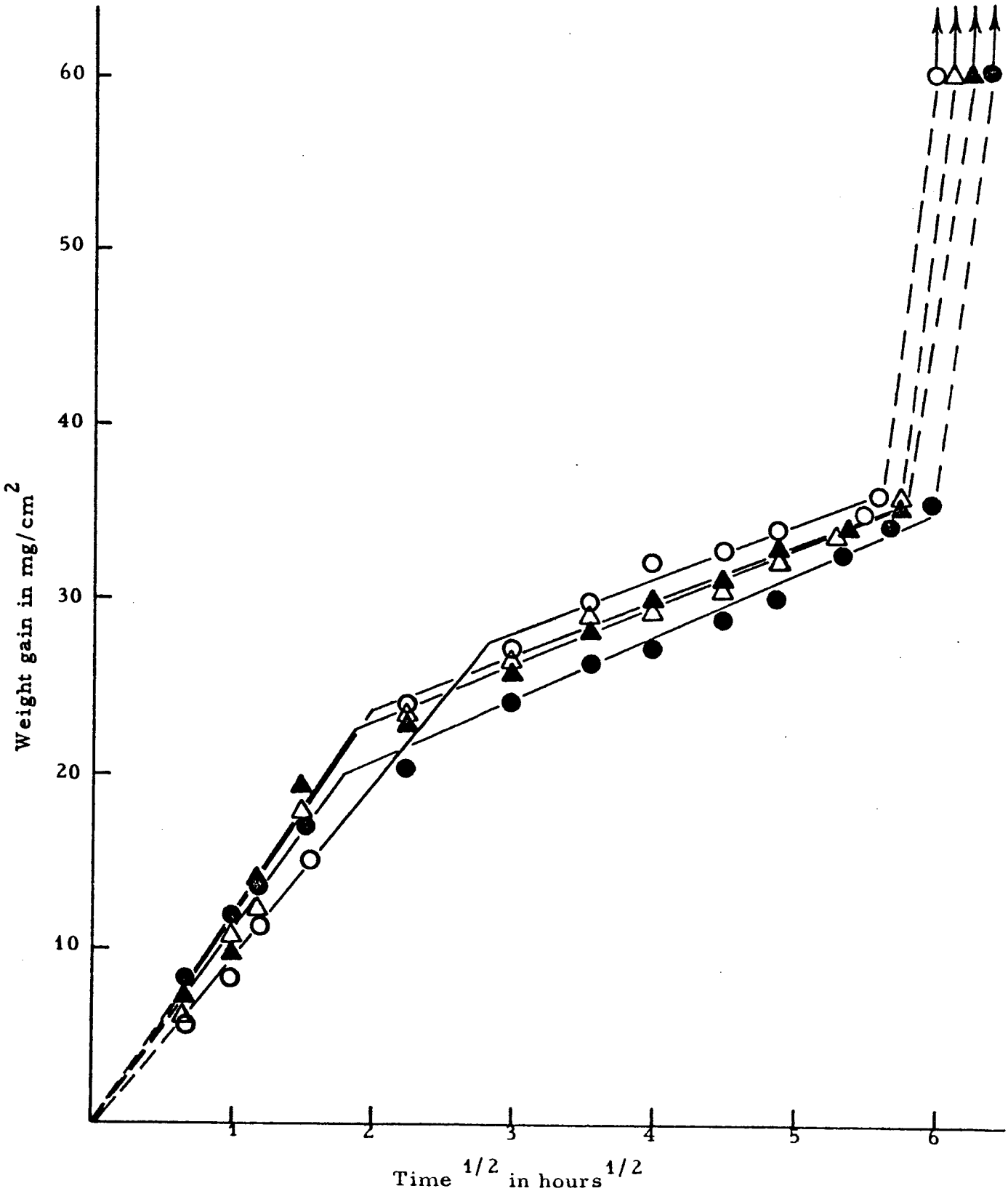

Fig. 7. The weight gains in dry air of 9.3 w/o Zr-Sn alloy samples expressed as a function of oxidation time at 990°C (○,●) and 1030°C (△,▲).

$$X^n = kt,$$

where X is the oxide thickness or weight gain per unit area

n is the reaction index

and t is the time.

The rate constants for the protective growth of the three oxides from liquid tin and solid parent metal substrates are presented in Figs. 8, 9 and 10. The agreement between the various sets of data is good and therefore suggests that the effect of the liquid substrate is to prolong the conditions under which the low-temperature growth mechanism is operative. This is an important inference since parabolic oxidation of zirconium and thorium has been reported to occur at temperatures substantially above those at which breakaway occurs. However, the mechanism of oxidation is not the same at high as at low temperatures. Levesque and Cubicciotti, for example, reported that the low temperature parabolic oxidation process of thorium had an activation energy of 31 k cals/mole (the value derived in this work was 30 k cals/mole) while Gerds and Mallet found that the high-temperature parabolic oxidation process had an activation energy of 62 k cals/mole.

Although there is reasonable agreement between the rate constants of the various sets of data plotted in the three figures, the values of the reaction index are at variance. The index was found to be 2 for the growth of both HfO_2 and ZrO_2 from liquid tin substrates, but values of 2.3 and 1.5 to 3.5 have been quoted for the low-temperature protective growth of

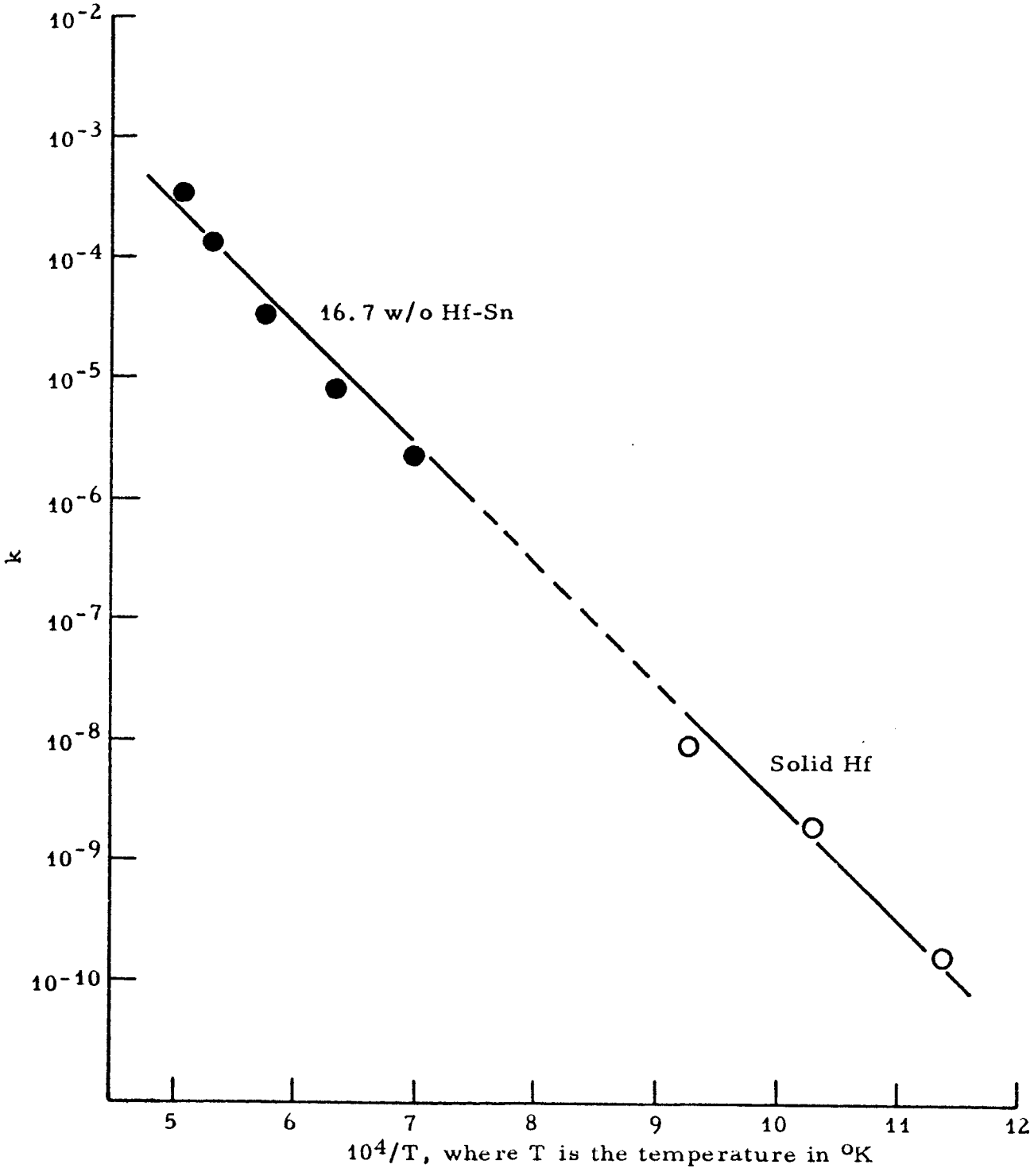

Fig. 8. The rate constants, k, for the growth of HfO_2 films on solid Hf and liquid Sn-16.7% Hf alloy samples exposed to air at various temperatures.

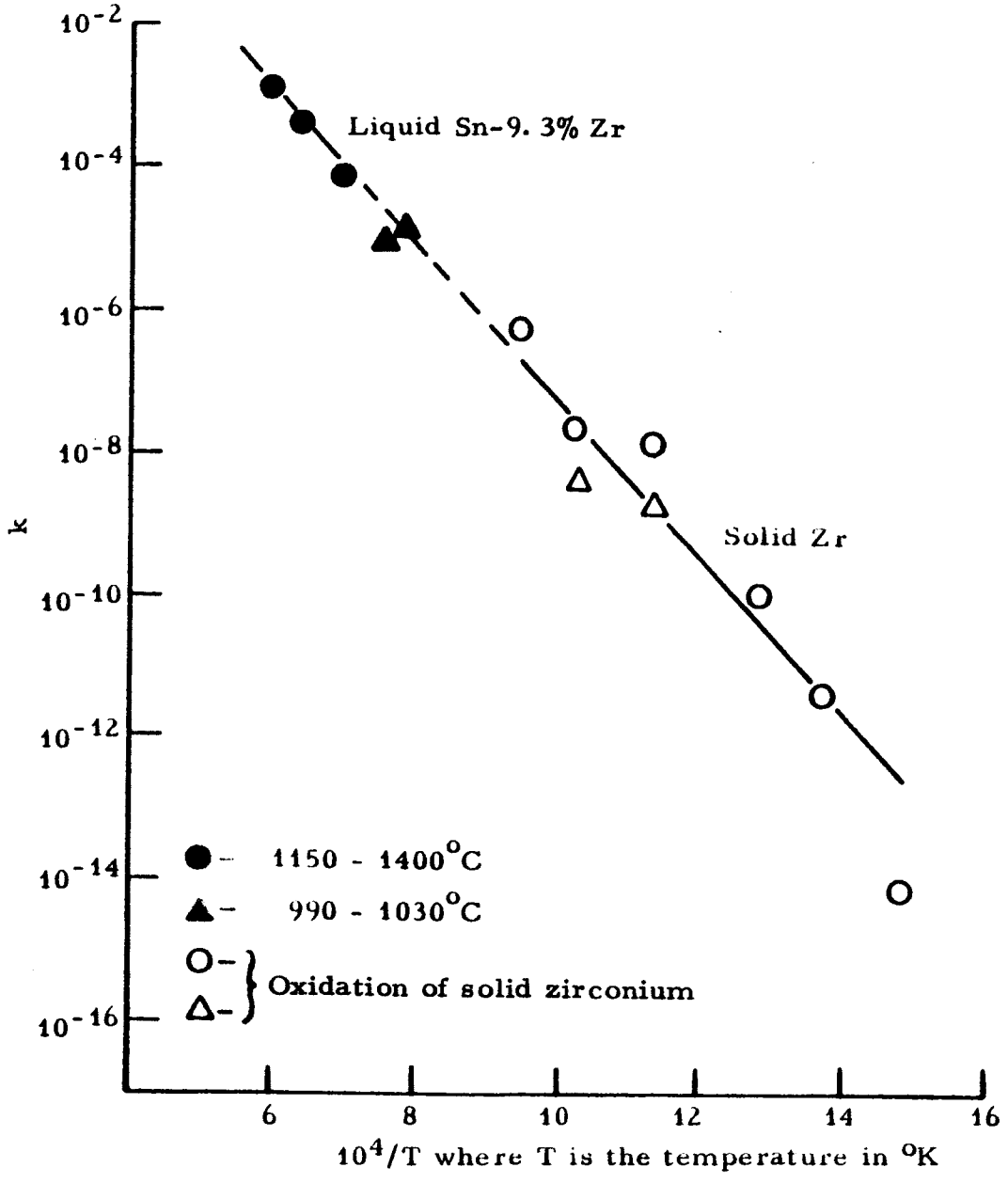

Fig. 9. The rate constants, k, for the growth of protective ZrO_2 films on solid Zr and a liquid Sn-9. 3% Zr alloy exposed to air at various temperatures.

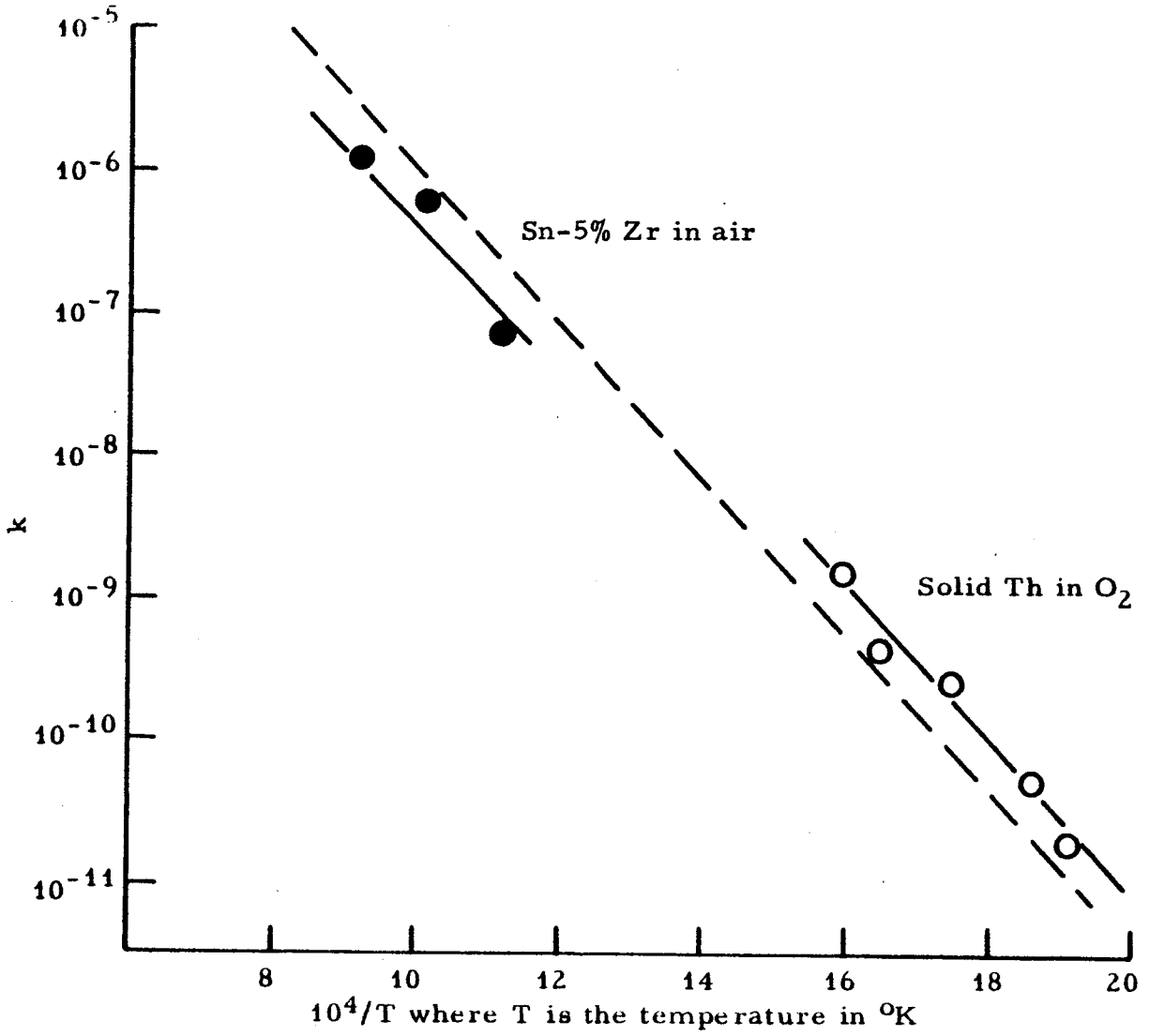

Fig. 10. The rate constants, k, for the oxidation of solid Th and a liquid Sn-5. 3% Th alloy.

HfO_2 and ZrO_2 from their solid parent metals. It is difficult, however, to decide whether this difference is of any major significance since variations in the reported values are so large. High reaction index values are usually associated with a significant influence of interfacial processes on the growth of oxide films. If it is assumed that the values derived in this work are indeed lower than those quoted in the literature for solid substrates, it can be deduced that the use of liquid substrates reduces the influence of interfacial processes. The data, however, are not precise enough to make such a deduction more than mere speculation.

Having discussed the major conclusions that can be drawn from the experimental data, it is possible to evaluate the relevance of this work to future coating programs. High-temperature parabolic growth oxides from liquid substrates has been demonstrated before and used by Sama and Lawthers in the development of a successful coating system;[5] however, the oxide (Al_2O_3) grown in that work, is not notably breakaway prone. The demonstration provided by this work that breakaway can be prevented or markedly delayed in the growth of breakaway-prone oxides such as ZrO_2 and HfO_2 now makes it possible to consider use of these oxides in protective coating systems. The utilization of this improvement under actual service conditions should be studied to prove that a wider choice of potential high-temperature coating systems is possible. This duplication, however, would not lead immediately to the development of new coating systems. The

high-temperature parabolic growth rates of HfO_2 and ZrO_2 are greater than those of Al_2O_3 and extrapolation of the present data to 2000°C (Fig. 11) indicates that the rates are probably greater than the tolerable maximum for a high temperature coating. These rates of diffusion controlled growth, therefore, will have to be reduced before practical coating systems can be developed.

Before concluding this discussion, it must be emphasized that it is not believed that any and every breakaway-prone oxide can be caused to grow as a protective film if a liquid substrate is used. An improvement can be expected if stresses at the oxide-metal interface are the cause of breakaway, but this is not always the case. Thorium and magnesium are reported to burn at moderate temperatures and, although some delay has been achieved by use of a liquid thorium-tin alloy, it seems unlikely that ThO_2 and MgO can be grown as protective films at 2000°C. Although not a refractory oxide forming material, liquid tin also fails to form protective films at 1000°C and above. The use of a liquid substrate, therefore, can not guarantee protective film growth for all cases. Nevertheless, it is believed that the use of a liquid substrate can markedly delay the onset of breakaway for the many systems in which breakaway is due to stresses or strains at the oxide-metal interface.

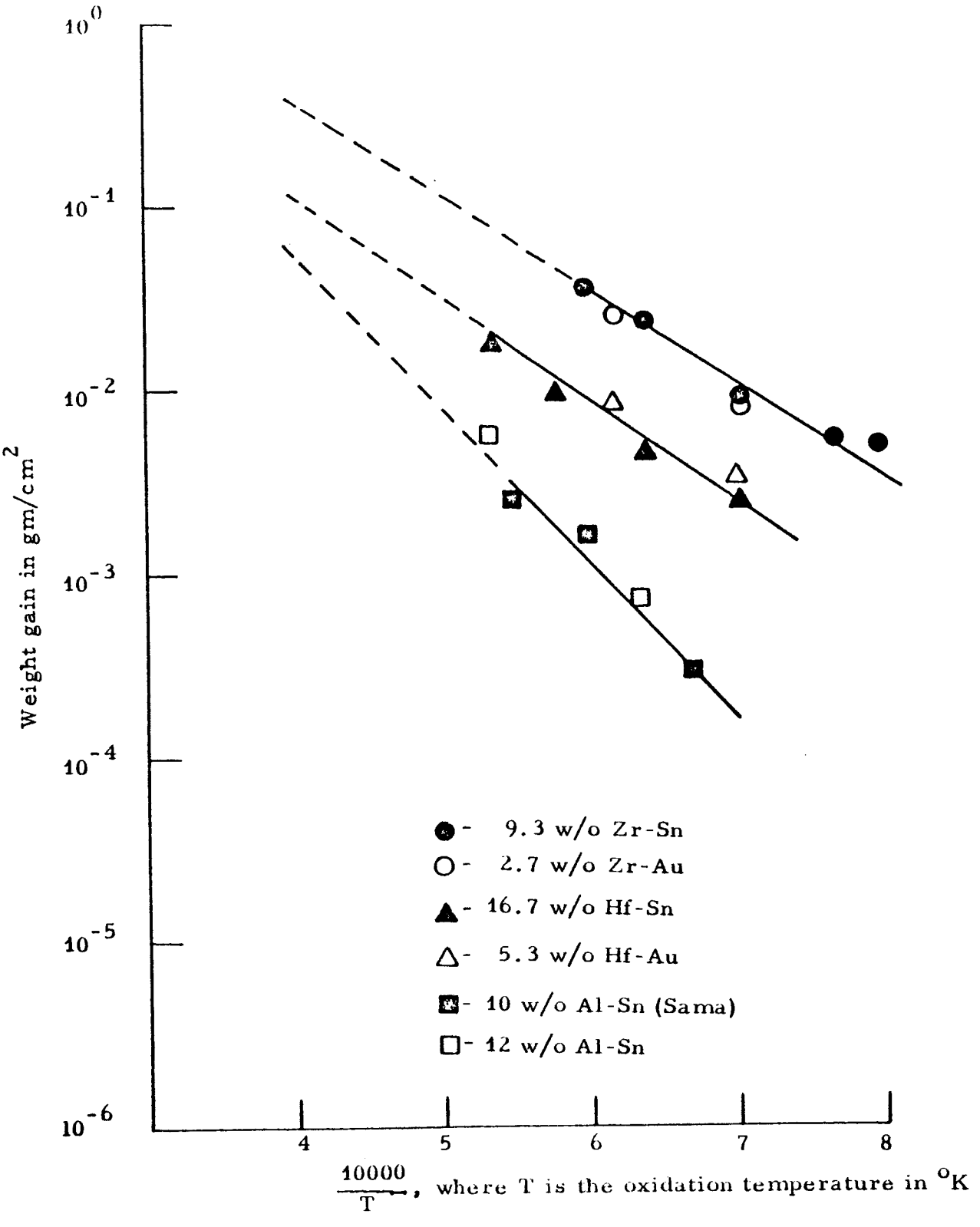

Fig. 11. The extent of oxidation produced by exposing five liquid alloys for one hour at various temperatures.

3. TERNARY DIFFUSION IN THE Zr-Th-O SYSTEM

Most of the successful protective coating systems developed to date depend on an intermetallic compound, diffusion bonded to the substrate, as a reservoir for the formation of a protective oxide. The success of such a coating depends primarily on the ability to form a specific oxide which is protective of the several oxides possible in a given system. The importance of diffusion processes is indicated by the results obtained in the study on silicide pest; the formation of tungsten and silicon oxides are associated with the low temperature, rapid failure.

For a pure metal, the phase sequence of the oxide layers produced on the surface can be predicted from the appropriate phase diagram by simply drawing an isothermal line. The only influence of diffusional processes is to determine the rates of growth of the various layers. With an alloy or intermetallic compound, however, the phase sequence or morphology cannot be predicted on the basis of the phase diagram or thermodynamic data since the relative diffusion rates of the three components of the system (oxygen, metal A and metal B) influence both the compositions of the oxides produced and the morphology of the layers which grow. The oxidation of several binary systems (Th-Zr-O, W-Hf-O and Zr-Y-O) are being investigated to provide further information on the behavior in the growth during oxidation to form fractory oxides of the specific compositions or crystal structure. Some in-

sight is being sought on the influence of the ternary equilibrium diagram, thermodynamics and relative diffusion rates on the behavior analyzed by analysis of the results as a ternary diffusion process. Work is progressing on all three systems mentioned, and the experimental work accomplished to date on the Th-Zr-O system permits some specific conclusions with regard to this system and general conclusions on the analysis of multicomponent oxidation as a ternary diffusion process. These results have implications in the problems of protecting tungsten (and other refractory metals); therefore a brief description of the results obtained to date on the Zr-Th-O system and a discussion of these results are presented.

3.1 EXPERIMENTAL PROCEDURE

Coupons of four Th-Zr alloys containing 30, 55, 70 and 85% thorium were made from mixtures of the Th and Zr powders in appropriate ratios. After blending, the powders were compacted and sintered in a vacuo for one hour at 1300°C. The compacts were arc melted in argon and homogenized by a vacuum anneal for 20 hours at 1200°C. The buttons produced were cold-rolled into strips 0.075 in. thick, with intermediate and final vacuum anneals of five hours at 1200°C. The strips produced were cut into 1/2-in. x 1/4-in. coupons and 1/16-in. diameter holes were drilled near one end. The coupons were then annealed for 5 hours at 1200°C before oxidation testing.

All oxidation tests were made in dry air. The Pt-Rh resistance-wound furnaces described by St. Pierre [6] were used. The solid specimens

were suspended in the furnace by 30% Rh-Pt rods passed through the drilled holes and placed across the top of an Al_2O_3 crucible. Liquid specimens, i.e., the 55, 70 and 85 w/o Th-Zr alloys at 1600°C, were premelted in argon prior to being exposed to air. Both weight gains and oxide thickness measurements were used to determine the extent of oxidation, but greater reliance was placed on thickness than weight gain measurements if both values were obtained. Selected samples were submitted to Battelle Memorial Institute for detailed X-ray and electron microprobe studies as follows:

1. Zr-30%Th alloy oxidized 1/2 and 2 hours at 1200°C and oxidized 20 minutes at 1400°C
2. Zr-55%Th oxidized 1/2 hour at 1200°C
3. Zr-85%Th alloy ozidized 1/2 and 2 hours at 1200°C

The procedure used at Battelle Memorial Institute is given in detail in the Appendix of the Second Progress Report [3]. The general procedure used, however, was to identify the composition of the phases observed in a metallographic cross-section of the specimen by microprobe analysis. The Zr and Th contents were obtained simultaneously, and the composition and the distance from the external surface of the analysis were determined. X-ray diffraction studies of the surface of the specimen and surfaces exposed by removing successive thicknesses gave a similar identification of the structure of the phases as a function of distance from the external interface. In this manner, it was possible to identify the phases formed in various layers and as well to determine the composition of these phases.

3.2 RESULTS

The rate of oxidation was determined by measuring the weight gain of the specimens after exposure at 750, 1000, 1200, 1400 and 1600°C. The results for each alloy were plotted as shown in Fig. 12 for the Zr-85%Th. The log of the specific weight gain is plotted as a function of the log of time and the reciprocal of the slope of the resulting curve is the index of reaction, n, in the equation

$$\left(\frac{\Delta W}{A}\right)^n = kt \qquad (1)$$

In almost all cases, the data for both noncyclic and cyclic tests for a given temperature and composition are well described by a straight line with a slope of 1 or 2, indicating nonprotective (linear) or protective (parabolic) film growth, respectively. The rate constants presented in Table II were determined from the straight lines of $\Delta W/A$ vs $\overline{t^{\frac{1}{n}}}$ plots by assuming that either linear (n=1) or parabolic (n=2) growth best describes the kinetics of the oxidation reaction.

At 750 and 1000°C linear oxidation was observed on all compositions tested, and the oxide formed was externally cracked. The tests were sequential cyclic runs on one sample, but spalling apparently occurred even on the first run as indicated by the fact that for the alloys containing 70-85%Th, the weight gained at 1000°C in the initial run is greater than that gained at 1200°C in the same time.

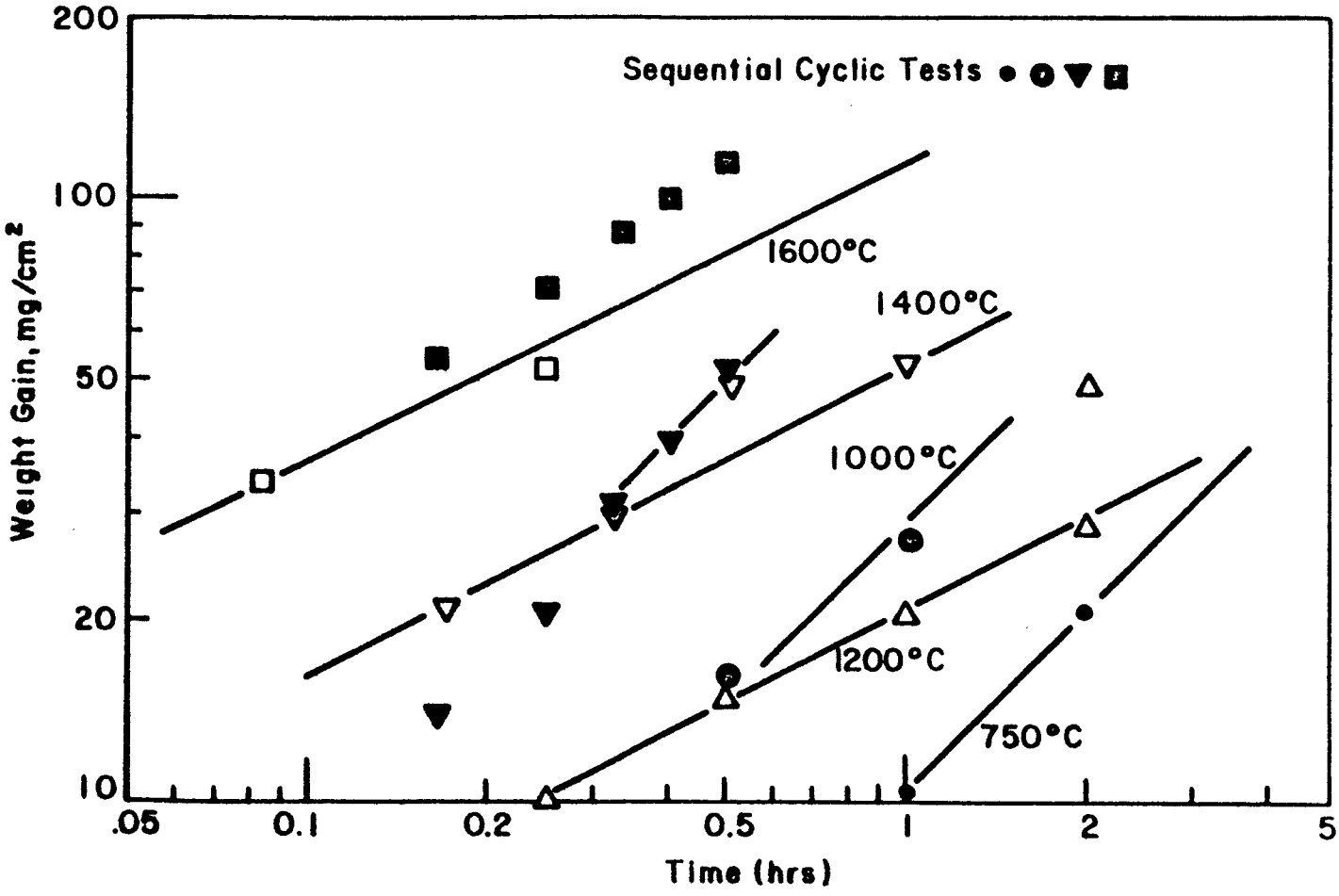

Fig. 12. Weight gained in oxidation of Zr-85%Th sheet in dry air.

TABLE II

The Effect of Temperature and Composition on the Growth Rate in Oxidation of Zr-Th Alloys at 750°C to 1600°C

	Zr-30% Th		Zr-55% Th		Zr-70% Th		Zr-85% Th	
Temp. (°C)	K_l^* gm/cm^2/hr	K_p^{**} gm^2/cm^4/hr	K_l^*	K_p^{**}	K_l^*	K_p^{**}	K_l^*	K_p^{**}
750	2.4×10^{-2}	--	1.5×10^{-2}	--	2.3×10^{-2}	--	2.2×10^{-2}	--
1000	4.2×10^{-2}	--	5.7×10^{-2}	--	5.2×10^{-2}	--	2.9×10^{-2}	--
1200	--	3.14×10^{-3}	--	9.6×10^{-4}	--	4.3×10^{-4}	--	4.3×10^{-4}
1400	--	3.2×10^{-2}	--	6.7×10^{-3}	--	1.6×10^{-3}	--	2.92×10^{-3}
1600	1.7	--	(2.2×10^{-1})	1.02×10^{-2}	--	6.10×10^{-3}	--	1.3×10^{-2}

$^*K_l$ = linear growth rate constant, i.e., $n \cong 1$ in $n \log \frac{\Delta W}{A} = \log Kt$.

$^{**}K_p$ = parabolic growth rate constant, i.e., $n \cong 2$ in $n \log \frac{\Delta W}{A} = \log Kt$.

At 1200°C individual specimens were used for each test and the data can be represented by a line with a slope of 1/2 indicating parabolic growth. The scales appeared to be sound and dense, and the edges and corners were intact in most cases; a sharp corner was retained in the oxide.

At 1400°C both cyclic and individual tests were run,and in the Zr-30Th and Zr-55Th alloy, a line with a slope of 1/2 describes the results of both types of tests. In the Zr-70%Th alloy at 1400°C, the weight gains for individual specimen tests indicated a slope of 1/2, but in sequential tests beyond 0.25 hours the slope changes toward a linear rate, indicating breakaway. In the Zr-85%Th alloy only the individual tests fit a slope of 1/2; the cyclic results indicate breakaway oxidation with a slope of 1. The external appearance of the oxides formed at 1400°C was similar to that observed at 1200°C.

At 1600°C only the Zr-30%Th alloy is solid at temperature. In the noncyclic tests, the rate of weight gain on the liquid Zr-(70-85%)Th alloys is parabolic, but slopes of 0.68 were obtained for cyclic tests. In the solid Zr-30%Th alloy only cyclic tests were run, and a slope of 1 was observed. The results of oxidation of the Zr-55%Th alloy was described by a curve with an initial slope of 1/2 and a slope of 1 for times greater than 0.25 hr. The oxides formed at 1600°C appeared to be dense and sound, but on standing at room temperature the oxides formed on the liquid alloys disintegrated in the atmosphere to form a very fine powder.

3.2.1 Structure of the Surface Layers

3.2.1.1 Metallographic Studies

Metallographic examination reveals that at 750 and 1000°C, oxidation of all alloys proceeds by linear nonprotective growth and the oxide formed contains a large number of cracks parallel to the surface of the specimen, as indicated in the first Quarterly Report.[3] Examination of the metallic substrate of specimens oxidized at 750°C indicates no change in substrate structure, and microhardness tests indicate no increase in hardness of the metal adjacent to the metal-oxide interface. Thus the amount of oxygen which penetrates or dissolves in the substrate must be relatively small. At 750 and 1000°C, breakaway due to fracture of the oxide is evidently the controlling process in the rate of oxidation. Oxygen permeates through the cracks to the metal-oxide interface, forming new oxide which, in turn, spalls and does not protect the substrate. Under these conditions, the substrate is oxidized essentially in situ and solid-state diffusion processes do not control the composition of the oxide layer.

Cross-sections through the surface layers of samples that exhibited parabolic growth at 1200 and 1400°C were studied. The thickness of the layers formed were measured and the microstructures after 1 hour in air at 1200°C in Fig. 13 are typical of the structures observed. Photomicrographs of the structures of the Zr-30%Th and Zr-85%Th alloys after 2 hours at 1200°C (Fig. 14) exhibit similar structures.

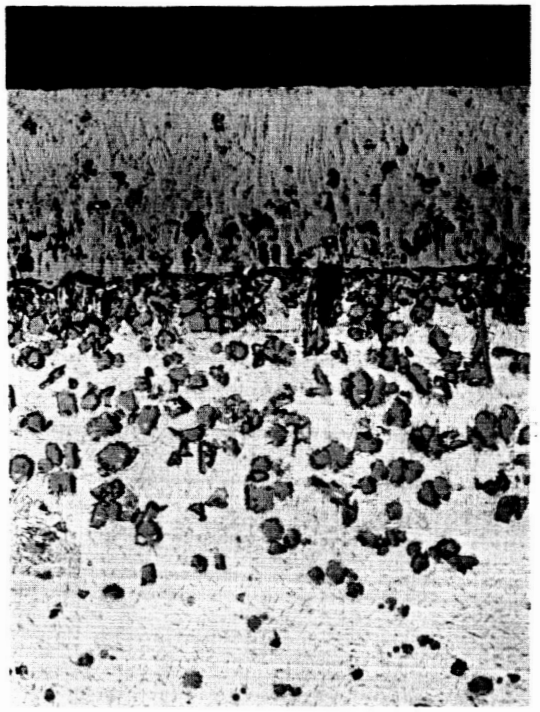

(a) 30 w/o Th. 100X

(b) 55 w/o Th. 250X

(c) 70 w/o Th. 250X

(d) 85 w/o Th. 250X

Fig. 13. The surfaces of thorium-zirconium alloys exposed to air for 1 hour at 1200°C.

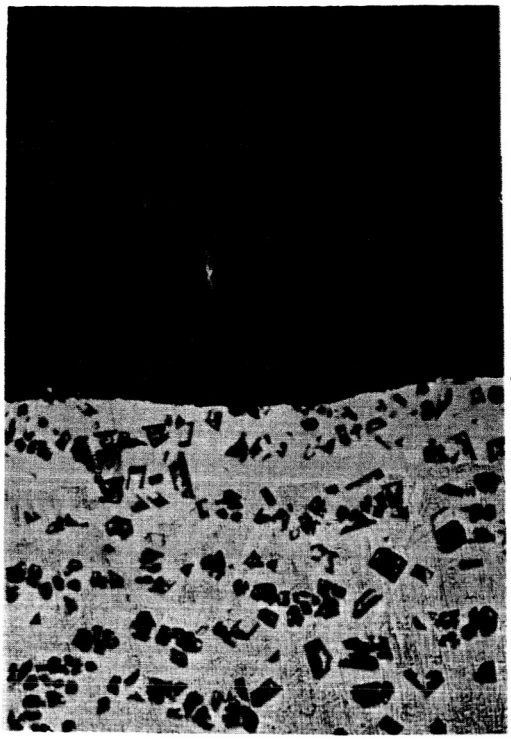

$ThO_2 + ZrO_2$

α Zr + ThO_2

$(\alpha + \alpha')$ Zr + ThO_2

Zr – 30 % Th

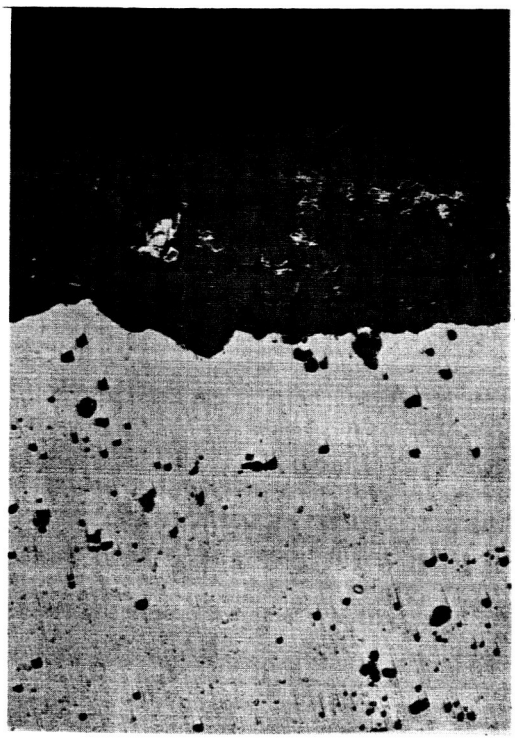

$ThO_2 + ZrO_2$

Th-Depleted Zr

Zr-Th Alloy

Zr – 85 % Th

Fig. 14. The effect of alloy content on the sequence of phases observed in Zr-Th samples oxidized in air for 2 hours at 1200°C. (100X)

In general, two types of structures were observed in samples oxidized at 1200 and 1400°C. At 1200 and 1400°C, the rate of growth is apparently diffusion-controlled in all compositions and compact adherent oxides are formed; however, the layers and structures observed in the Zr-30%Th and Zr-55%Th alloys (thorium lean) differ from those in the Zr-70%Th and Zr-85%Th (thorium rich) alloys. In the thorium lean alloys, several layers which thicken with time are observed as follows:

1. An external two-phased oxide;
2. An internally oxidized layer consisting of a single-phase metal matrix containing oxide particles;
3. A transformed two-phase metal matrix containing oxides formed by internal oxidation.

Hardness traverses of the metal + oxide layer observed beneath the oxide in the thorium lean alloys were made on alloys oxidized at 1200 and 1400°C. The single-phase matrix structure has a hardness above 1000 VHN near the oxide-metal interface, and in its entirety is harder than the substrate from which it is formed. The transformed metal + oxide layer is similarly harder than the substrate.

All of the layers thicken with time, and in the Zr-30%Th alloy, which was oxidized 30 minutes at 1400°C, the internally oxidized zone (layer 3) penetrated almost to the centerline of the specimen. In this sample large fissures in layer 2 and in the corners of the outer oxide layer were

observed. The oxide was grossly distorted by growth, but cracks were observed only at corners and in the regions of the support hole in the specimen. In specimens oxidized at shorter times at 1400°C or equivalently shorter time at 1200°C, the corners were essentially intact and formed a sharp corner angle at about 90°.

In the Zr-70%Th and Zr-85%Th alloys, the external oxide is the only layer which grows appreciably, and the rate of growth is considerably less than the rate in the thorium-lean alloys. Some indication of a small amount of internal oxidation at 1200°C may be present in the Zr-70%Th alloy structure (Fig. 13); however, internal oxidation and the solution of oxygen in the metallic matrix do not occur to an appreciable degree in the thorium-rich alloys. No single-phased region in the metallic matrix is observed, and hardnesses immediately adjacent to the metal-oxide interface indicate no hardening from oxygen solution.

At 1600°C observations were complicated by the fact that only the Zr-30%Th alloy was solid at temperature. In addition, the scales that formed on the liquid alloys were initially sound and nonporous but rapidly disintegrated at room temperature so that microstructure observations were not made. However, the disintegrated scales were analyzed by X-ray diffraction to determine their structure, and the following results were obtained:

Zr-55%Th: ThO_2 + 10%ZrO_2 + (ZrN detected $\leq$ 5%)

Zr-70%Th: ThO_2 + $\leq$ 5% [ZrN]; (ZrO_2 possibly detected < 5%)

Zr-85%Th: ThO_2 + $\leq$ 5% (ZrN + several unidentified lines - trace ZrO_2 ?)

The oxide that forms at 1600°C on the liquid alloys is predominantly ThO_2. The ZrO_2 observed in the Zr-55%Th alloy may have formed after the composition being oxidized was partially solid. These results indicate that thermodynamic considerations are overriding in the oxidation of the liquid alloys. Chemical analysis of the residual metal of Zr-55%Th samples oxidized for 15 and 30 minutes at 1600°C indicated thorium contents of 45 and 46.7% respectively. An alloy containing 45% thorium would be partly solid at 1600°C, and microscopic examination indicated localized areas where internal oxidation and an oxygen-saturated zone had formed, similar to that observed in the oxidation of the solid alloy.

3.2.1.2 Microprobe and X-ray Diffraction Studies

Microprobe analysis and X-ray diffraction studies of alloys oxidized at 1200 and 1400°C are included in Appendix A of Ref. 3. Several conclusions can be drawn from the results which have direct bearing on the rationalization of the oxidation processes at 1200 and 1400°C. By combining the microprobe, X-ray, metallographic and microhardness results, it is possible to describe the layers formed with greater accuracy, and even

to assign approximate zirconium and thorium ratios of the phases observed. For example in the Zr-30%Th and Zr-55%Th alloys (14 a/o and 31 a/o Th respectively), the sequence of phases at 1200°C observed in order from the external surface towards the center of the sample are as follows:

Layer 1. ZrO_2 (<4 a/o Th) and ThO_2 (Zr content varies). Both cubic and monoclinic ZrO_2 are observed in the Zr-14a/o Th alloy, although the tetragonal phase is stable at temperature. ZrN is present as a discrete phase in the oxide.

Layer 2. ThO_2 (~50 a/o Zr) + α Zr (< 2 a/o Th and up to 30 a/o O_2).

Layer 3. ThO_2 (~30 a/o Zr) + α 1 β Zr (<3 a/o Th).

Layer 4. A solid-solution zone in which the ratio of thorium to zirconium in the metal increases from 5 a/o and 14 a/o Th to the original alloy compositions of 14 and 31 a/o Th respectively.

In the Zr-85%Th (69 a/o Th) alloy, the sequence of layers or phases and the approximate composition is as follows:

Layer 1. A thin external two-phased oxide (ZrO_2 and ThO_2). The composition of the discrete phases is not defined.

Layer 2. A layer of ThO_2 (X-ray results indicate no ZrO_2 present) which contains 20 a/o Zr (X-ray results indicate some ZrN

as a discrete phase, but the zirconium content in ThO_2 is uniformly high).

Layer 3. A metallic substrate in which the thorium content increases from ~24 a/o Th at the metal-oxide interface to the matrix composition (69 a/o Th).

3.3 DISCUSSION OF RESULTS

The rates of oxidation at 1200, 1400 and 1600°C of the Zr-Th alloys are compared with previously determined rates of formation of ZrO_2 on liquid Zr-Sn alloys and ThO_2 on Th-Sn alloys in Fig. 15. At 1600°C, the parabolic rate constant for the alloys is located directly between the rate constants for the oxidation of Zr and Th in Sn alloys. At 1200° and 1400°C the rates observed for the Zr-30Th and Zr-55Th alloys are considerably higher than a straightline average of the rates for Th and Zr in Sn. This suggests that the occurrence of internal oxidation is important in determining the overall rate constant for these alloys. The rate constants for the Zr-70% alloy at 1200 and 1400°C, and for the Zr-85%Th alloy at 1200°C are between the rate constants for the oxidation of pure Th and Zr. This indicates that the rates observed are an average of the rates determined by the diffusion of oxygen through the Zr and Th-rich two-phase oxide.

Internal oxidation eventually does lead to failure by breakaway in the Zr-30Th and Zr-55%Th alloys but the spalling occurs first in the oxygen-saturated Zr which leads to cracking of the oxide at the ends of the specimens.

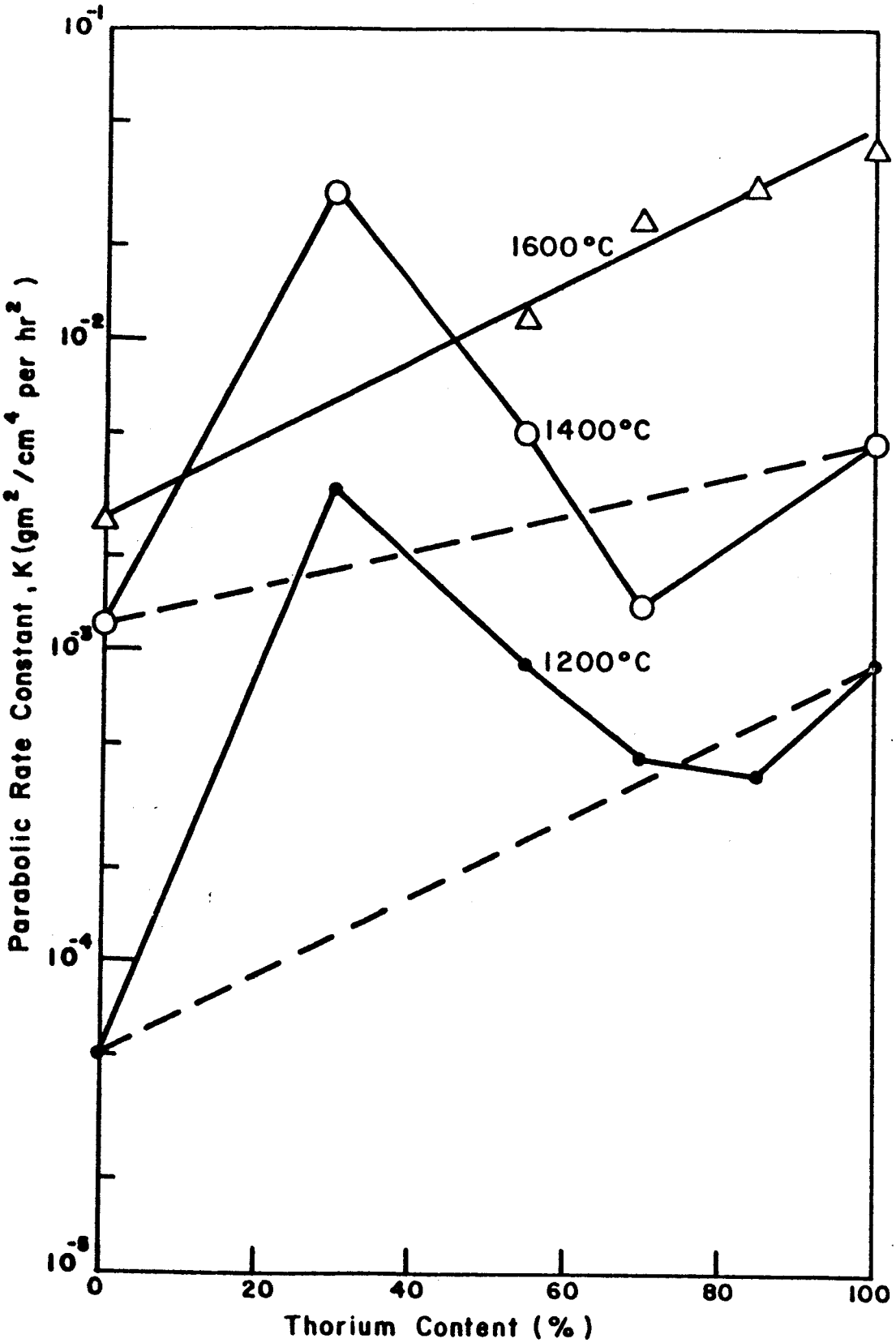

Fig. 15. The effect of thorium content on the parabolic rate constant in oxidation of Zr-Th alloys at 1200 to 1600°C. (Parabolic rates for Zr and Th obtained by interpolation or extrapolation.)

The most surprising fact is that the oxide does not spall in most of the alloys, even though the oxidation process causes a 10% or more increase in the thickness of the specimen. Even the corners of the specimen after 10% increase in thickness are essentially sound, with no indication of corner cracking in spite of the fact that the oxide is apparently being formed by anion diffusion at the metal oxide interface. The fact that the oxide can undergo such distortion without cracking indicates that the two-phase structure of thoria surrounded by a mixture of zirconia or zirconia plus thoria-rich oxides, has considerable ductility at temperatures of 1200°C and above.

If the growth of each layer observed after oxidation at 1200 to 1400°C is truly diffusion-controlled, then all layers should thicken with time, according to equation (1) where $n = 2$ and k is a different constant for each layer. The weight gain should be directly related to the rate of thickening of each zone and to the total thickness. In a plot of the weight gain versus the thickness of the oxide layer, and the oxide layer plus internally oxidized zone, linear relationship is obtained for both at 1200 and 1400°C. The thickness of the oxide layer for a given weight gain is independent of temperature, indicating that the oxide density (and probably composition) does not change with temperature. The thickness of the internally oxidized zone does change with temperature, the layer being thicker for a given weight gain at 1200°C than at 1400°C. In the thorium-rich alloys, only the oxide layer grows with time, and the thickness of the

oxide for a given weight gain is increased which is consistent with the fact that practically all of the oxygen is in the oxide layer in the thorium-rich alloys.

3.3.1 Structure of Surface Zone

In order to discuss the sequence of phases at the air-coating interface in terms of the "ternary-diffusion" concept, it is first necessary to construct a tentative phase diagram for the Th-Zr-O ternary system. The Zr-Th and Zr-O binary diagrams are known and the quasibinary ZrO_2-ThO_2 diagram is also known. The Th-O diagram is not known, but the existence of oxide particles in a melted thorium button containing 1500 ppm O_2 suggests that the solubility of oxygen in thorium is extremely low.

The metallographic, hardness, X-ray diffraction and microprobe results of alloys oxidized at 1200°C define the zirconium-thorium ratio of the phases observed and the structure at temperature or structures which result from transformation on cooling, and permit an estimate of the oxygen gradient in the substrate. These results have been used to construct the tentative 1200° isotherm shown in Fig. 16. The cubic zirconia found in the oxide of the Zr-30%Th alloy has not been included in this diagram since Roy and Mumpton [7] have shown that the cubic zirconia observed in ThO_2-ZrO_2 alloys is a metastable rather than stable phase. It is not known whether the metastable phase is formed at temperature or on cooling, but

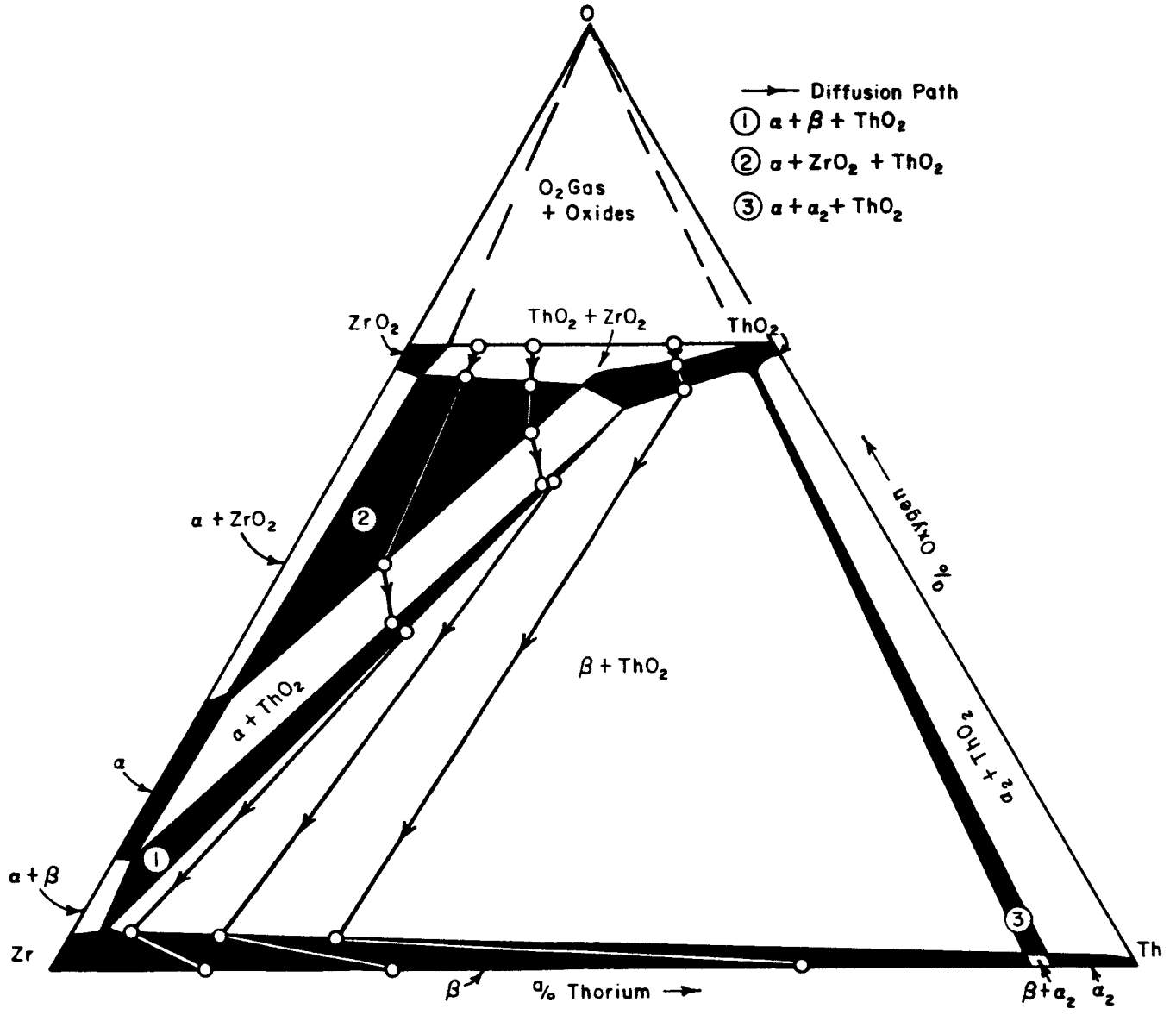

Fig. 16. Tentative phase diagram at 1200°C of Th-Zr-O system based on microprobe, x-ray and microstructure observations in oxidation of three Zr-Th alloys. Composition paths for oxidation of 3 Zr-Th alloys are indicated by arrowed lines.

a three-phased region should not be observed unless one of the phases is metastable.

The low solubility of thorium (<2 a/o) in the oxygen-rich internally oxidized zone of the Zr-14 a/o Th and Zr-31 a/o Th alloys helps to establish the oxygen gradient since the oxygen content of the zirconium-oxygen phases at the limit of solubility of thorium in these phases should not differ greatly from that in the Zr-O binary diagram. The low thorium content between the substrate and the internally-oxidized interface, and the identification of the internal oxide as ThO_2 suggests that the $\beta + ThO_2$ two-phase region exists at very low thorium and oxygen contents. Finally, the high zirconium contents of the ThO_2 in the $\alpha + ThO_2$ and $\beta + ThO_2$ internally oxidized layers in the thorium-lean alloys was used to construct the extended ThO_2 single-phase region with the assumption that this region is qualitatively only slightly oxygen-lean. The three-phase regions were observed as boundaries between layers. The $\alpha_2 + \beta + ThO_2$ and $\alpha_2 + ThO_2$ regions were not encountered in the diffusion couples but must exist at 1200°C.

The tentative diffusion paths of the Zr-14 a/o Th, Zr-31 a/o Th and Zr-60 a/o Th alloys at 1200°C are also indicated in Fig. 16. In the Zr-14 a/o Th and Zr-31 a/o Th alloys the composition paths cross tie lines in the $ThO_2 + ZrO_2$, $\alpha Zr + ThO_2$ and $\beta + ThO_2$ two-phase regions, and thus the internally oxidized layers as well as the two-phased oxide layer is observed in the microstructure. A net material flow of thorium from the unaltered

substrate to form the thorium-lean metallic zone and oxide phases richer in thorium is apparent in all alloys.

In the Zr-69 a/o Th alloy the composition path through the $\beta + ThO_2$ region is also a tie line so that the two-phase region is observed as a boundary between the oxide and substrate rather than an internally oxidized zone. The external layer of the oxide is two-phased ThO_2 and ZrO_2 since tie lines are crossed. The existence of a single-phase zirconium-rich ThO_2 solid solution agrees with the microstructure and initial microprobe results. Although ZrO_2 is observed by X-ray diffraction only in the outer portion of the scale, the presence of large amounts of zirconium in the oxide formed indicates that a layer of single-phase oxide exists in the oxidized specimen. However, further experiments are needed to verify the existence of the zirconium-rich ThO_2 oxide. Nitrogen has been ignored in the analysis of the specimens even though zirconium nitride has been detected in the oxide scales formed.

The diffusion paths and phase diagram in Fig. 16 are reasonably consistent, and speculation on the kinetics of diffusion in certain cases is possible. In the Zr-14 to 31 a/o Th alloys, the flux of thorium to the metal-oxide interface is not sufficient to combine with all of the oxygen, and as a net result, oxygen diffuses into the thorium-depleted metallic substrate until the solubility limit is reached for a given thorium-zirconium ratio. Thorium oxide nucleates and grows as an internal oxide until the

faster diffusing oxygen consumes the thorium available locally and diffuses into the substrate to nucleate additional ThO_2-rich particles at a point further removed from the surface of the specimen.

If this process is active in the Zr-30 to 55%Th alloys, the ratio of the diffusion of oxygen to the diffusion of thorium must decrease with increasing temperature, since the particles nucleate with greater frequency at the higher temperatures. The spatial density of internally oxidized particles in the substrate is greater at higher temperature, and the thickness of the internally oxidized boundary in relation to the thickness of the external oxide decreases with increasing temperature.

The most surprising result is that oxidation at 1200 to 1400°C occurs without breakaway even though stress is generated during oxidation. The corners of the specimens retain a sharp 90° angle, even after the oxide formed causes an increase in thickness of 10% or more. These results indicate that the oxide can accommodate large strains at 1200 to 1400°C without cracking, and thus prevent breakaway or spalling of the oxide which would lead to linear oxidation.

The nonprotective growth of oxides over the alloys at 1000°C and 750°C can now be rationalized if the strains which must be accommodated at the metal-oxide interface during the growth of the oxide are considered. The spalling of the oxide at 750 and 1000°C seems to be the direct result of poor ductility in the two-phase oxides at these temperatures.

The strains due to growth at the metal-oxide interface cause high shear and tensile stresses in the oxide which cause fracture at 750 and 1000°C but apparently cause deformation without cracking in the two-phase oxide at higher temperatures.

4. CONCLUSIONS

The results of our work to date on the oxidation of Zr-Th alloys have led to the following conclusions:

1. Oxidation at temperatures from 750 to 1000°C is linear due to the spalling of the oxide formed, which results from the generation of mechanical stresses during the growth of the oxide.
2. Oxidation at 1200 to 1400°C is diffusion-controlled, and the films formed are compact and adherent.
3. Oxides formed at 1200°C and above accommodate thickness increases of 10% or more without cracking or breakaway oxidation.
4. The rates of diffusion-controlled oxidation are considerably higher for alloys that form internally oxidized zones than for alloys that do not.
5. Insofar as the limited data on diffusion paths and phase diagram are valid:

a. the composition paths in the ternary phase diagram do not cross.

b. two-phased structures are observed when tie lines are crossed, but not when the diffusion path follows a tie line.

c. the morphology and existence of a two-phased internally oxidized zone depend upon the relative diffusion rates of the metals and oxygen, as well as the phase equilibria.

REFERENCES

1. M. Nicholas and C. D. Dickinson, "High-Temperature Protective Coatings for Refractory Metals", Part II, Sixth Meeting of the Refractory Composites Work Group, Dayton, Ohio, 1962.

2. M. Nicholas, A. L. Pranatis, C. D. Dickinson, "The Analysis of the Basic Factors Involved in the Protection of Tungsten Against Oxidation," Part I, ASD-TRD-62-205.

3. M. G. Nicholas, C. D. Dickinson, and L. L. Seigle, "Experimental Study of Factors Controlling the Effectiveness of Oxidation of High Temperature Protective Coatings for Tungsten", First and Second Progress Reports on AF 33 (657)-8787, August 15 and November 15, 1962.

4. M. G. Nicholas and C. D. Dickinson, "An Analysis of the Basic Factors Involved in the Protection of Tungsten Against Oxidation," ASD-TRD-62-205, Part II, September 1962.

5. L. Sama and D. D. Lawthers, ASD Tech. Rep., 61-233

6. P. D. St. Pierre, Bull. of Am. Ceram. Soc., 39, p. 264, 1960.

7. F. A. Mumpton and R. Roy, "Low Temperature Equilibria Among ZrO_2, ThO_2 and UO_2," J. of the American Ceramic Soc., Vol. 43, 1960, p. 234.